Tran-SET

Transportation Consortium of South-Central States

Solving Emerging Transportation Resiliency, Sustainability, and Economic Challenges through the Use of Innovative Materials and Construction Methods: From Research to Implementation

Use of Bagasse Ash as a Concrete Additive for Road Pavement Application

Project No. 18CLSU03

Lead University: Louisiana State University

Final Report

August 2019

Disclaimer

The contents of this report reflect the views of the authors, who are responsible for the facts and the accuracy of the information presented herein. This document is disseminated in the interest of information exchange. The report is funded, partially or entirely, by a grant from the U.S. Department of Transportation's University Transportation Centers Program. However, the U.S. Government assumes no liability for the contents or use thereof.

Acknowledgements

The authors would like to acknowledge the financial support for this study by the Transportation Consortium of South-Central States (Tran-SET) and the Louisiana Transportation Research Center (LTRC).

TECHNICAL DOCUMENTATION PAGE

1. Project No.	2. Government Accession No.	3. Recipient's Catalog No.
18CLSU03		

4. Title and Subtitle	5. Report Date
Use of Bagasse Ash as a Concrete Additive for Road Pavement Applications	Aug. 2019 **6. Performing Organization Code**

7. Author(s)	8. Performing Organization Report No.
PI: Gabriel Arce https://orcid.org/0000-0002-3610-8238 Co-PI: Marwa Hassan https://orcid.org/0000-0001-8087-8232 Co-PI: Maria Gutierrez-Wing https://orcid.org/0000-0002-3279-9123 Co-PI: Michele Barbato https://orcid.org/0000-0003-0484-8191	

9. Performing Organization Name and Address	10. Work Unit No. (TRAIS)
Transportation Consortium of South-Central States (Tran-SET) University Transportation Center for Region 6 3319 Patrick F. Taylor Hall, Louisiana State University, Baton Rouge, LA 70803	**11. Contract or Grant No.** 69A3551747106

12. Sponsoring Agency Name and Address	13. Type of Report and Period Covered
United States of America Department of Transportation Research and Innovative Technology Administration	Final Research Report Mar. 2018 – Mar. 2019 **14. Sponsoring Agency Code**

15. Supplementary Notes

Report uploaded and accessible at Tran-SET's website (http://transet.lsu.edu/).

16. Abstract

The objective of this study was to evaluate the use of sugarcane bagasse ash (SCBA) as a partial replacement of cement in concrete for road pavement application. The study explored the pozzolanic activity of SCBA produced from three different processing methodologies (i.e., raw SCBA, controlled SCBA and post-processed SCBA). The experimental results revealed that SCBA produced by the controlled burning of sugarcane bagasse fiber (SBF) at 650°C and grinding (C-650), presented the maximum pozzolanic activity. However, this SCBA production process was deemed challenging for large-scale industrial application due to low SCBA yield (i.e., 3 to 6%). On the other hand, post-processing of raw SCBA, by burning at 450°C and grinding (P-450), produced a similar pozzolanic activity to that of SCBA C-650. Moreover, since post-processing of raw SCBA produced a significantly higher SCBA yield (i.e., 85 to 90%) than that of controlled burning of SBF, SCBA P-450 was selected for further investigation in concrete mixtures. The effect of different dosages of P-450 (i.e., 20, 30, and 40% cement replacement by weight) on concrete properties was evaluated. It was determined that concrete mixtures utilizing substitutions of 10% and 20% of cement with SCBA exhibited a similar compressive strength to that of control after 90 days of curing for Class-A and Class-B concretes, respectively. At higher levels of cement replacement, the compressive strength of concrete mixtures decreased proportionally at both, 28 and 90 days of curing; yet, the relative strength gain from 28 to 90 days increased. Furthermore, at 90 days of curing, surface resistivity of SCBA admixed concrete mixtures was superior to that of control for all cases. Finally, a cost analysis showed that a 10% cement replacement with SCBA in concrete could yield a reduction of per lane-mile cost of 0.75%.

17. Key Words	18. Distribution Statement
Bagasse Ash, Concrete, Pavement	No restrictions. This document is available through the National Technical Information Service, Springfield, VA 22161.

19. Security Classif. (of this report)	20. Security Classif. (of this page)	21. No. of Pages	22. Price
Unclassified	Unclassified	42	

Form DOT F 1700.7 (8-72) **Reproduction of completed page authorized.**

SI* (MODERN METRIC) CONVERSION FACTORS

APPROXIMATE CONVERSIONS TO SI UNITS

Symbol	When You Know	Multiply By	To Find	Symbol
		LENGTH		
in	inches	25.4	millimeters	mm
ft	feet	0.305	meters	m
yd	yards	0.914	meters	m
mi	miles	1.61	kilometers	km
		AREA		
in^2	square inches	645.2	square millimeters	mm^2
ft^2	square feet	0.093	square meters	m^2
yd^2	square yard	0.836	square meters	m^2
ac	acres	0.405	hectares	ha
mi^2	square miles	2.59	square kilometers	km^2
		VOLUME		
fl oz	fluid ounces	29.57	milliliters	mL
gal	gallons	3.785	liters	L
ft^3	cubic feet	0.028	cubic meters	m^3
yd^3	cubic yards	0.765	cubic meters	m^3
		NOTE: volumes greater than 1000 L shall be shown in m^3		
		MASS		
oz	ounces	28.35	grams	g
lb	pounds	0.454	kilograms	kg
T	short tons (2000 lb)	0.907	megagrams (or "metric ton")	Mg (or "t")
		TEMPERATURE (exact degrees)		
^oF	Fahrenheit	5 (F-32)/9 or (F-32)/1.8	Celsius	^oC
		ILLUMINATION		
fc	foot-candles	10.76	lux	lx
fl	foot-Lamberts	3.426	$candela/m^2$	cd/m^2
		FORCE and PRESSURE or STRESS		
lbf	poundforce	4.45	newtons	N
lbf/in^2	poundforce per square inch	6.89	kilopascals	kPa

APPROXIMATE CONVERSIONS FROM SI UNITS

Symbol	When You Know	Multiply By	To Find	Symbol
		LENGTH		
mm	millimeters	0.039	inches	in
m	meters	3.28	feet	ft
m	meters	1.09	yards	yd
km	kilometers	0.621	miles	mi
		AREA		
mm^2	square millimeters	0.0016	square inches	in^2
m^2	square meters	10.764	square feet	ft^2
m^2	square meters	1.195	square yards	yd^2
ha	hectares	2.47	acres	ac
km^2	square kilometers	0.386	square miles	mi^2
		VOLUME		
mL	milliliters	0.034	fluid ounces	fl oz
L	liters	0.264	gallons	gal
m^3	cubic meters	35.314	cubic feet	ft^3
m^3	cubic meters	1.307	cubic yards	yd^3
		MASS		
g	grams	0.035	ounces	oz
kg	kilograms	2.202	pounds	lb
Mg (or "t")	megagrams (or "metric ton")	1.103	short tons (2000 lb)	T
		TEMPERATURE (exact degrees)		
^oC	Celsius	1.8C+32	Fahrenheit	^oF
		ILLUMINATION		
lx	lux	0.0929	foot-candles	fc
cd/m^2	$candela/m^2$	0.2919	foot-Lamberts	fl
		FORCE and PRESSURE or STRESS		
N	newtons	0.225	poundforce	lbf
kPa	kilopascals	0.145	poundforce per square inch	lbf/in^2

TABLE OF CONTENTS

TABLE OF FIGURES

LIST OF TABLES

ACRONYMS, ABBREVIATIONS, AND SYMBOLS

ANOVA	Analysis of Variance
ASTM	American Society for Testing and Materials
DOTD	Department of Transportation and Development
EDS	Energy Dispersive X-ray Spectroscopy
LOI	Loss on Ignition
LSU	Louisiana State University
LTRC	Louisiana Transportation Research Center
DOTD	Louisiana Department of Transportation and Development
OPC	Ordinary Portland cement
SAI	Strength Activity Index
SBF	Sugarcane Bagasse Fiber
SCBA	Sugarcane Bagasse Ash
SCM	Supplementary Cementitious Material
SEM	Scanning Electron Microscopy
XRD	X-ray Diffraction
XRF	X-ray Fluorescence

EXECUTIVE SUMMARY

The objective of this study was to produce the necessary engineering knowledge to bring sugarcane bagasse ash (SCBA) closer to implementation as a partial substitute for cement in concrete for road pavement application. The study explored the physical and chemical properties of SCBA produced from three different processing methodologies: (1) SCBA produced by the uncontrolled burning of sugarcane bagasse fiber (SBF) in the sugar factory, minimally processed by drying and sieving (i.e., raw SCBA); (2) SCBA produced by the controlled burning of SBF and grinding (i.e., controlled SCBA); and (3) SCBA produced by the post-processing (burning and grinding) of raw SCBA (i.e., post-processed SCBA); in order to determine an efficient production methodology yielding satisfactory pozzolanic activity of SCBA. A total of 11 different SCBA materials (1 raw SCBA, 5 controlled SCBAs, and 5 post-processed SCBAs) were prepared and characterized by Scanning Electron Microscopy (SEM), Energy Dispersive X-ray Spectroscopy (EDS), X-ray Fluorescence (XRF), X-ray Diffraction (XRD), particle size analysis, pH test and sulfate solubility test per ASTM D5239, and moisture content, loss on ignition (LOI) and Strength Activity Index (SAI) per ASTM C311. The experimental results revealed that raw SCBA is not suitable as a SCM due to its high carbon content and large particle size which limits its pozzolanic activity (SAI of 68.72%). Yet, all controlled and post-processed SCBAs evaluated in this study met ASTM C618 requirements for pozzolanic component, SAI, moisture content, LOI and SO_3 content. The SCBA produced by the controlled burning of sugarcane bagasse fiber (SBF) at 650°C for 3 hours (after 3 hours at 350°C) and grinding for 35 minutes using a jar mill at 300 rpm (i.e., SCBA labeled as C-650), presented the maximum pozzolanic activity with a SAI of 92.13%. However, this SCBA production process was deemed challenging for large-scale industrial application due to low SCBA yield (i.e., 3 to 6%). On the other hand, post-processing of raw SCBA, by burning at 450°C for 3 hours (after 2 hours at 350°C) and grinding for 35 minutes using a jar mill at 300 rpm (SCBA labeled as P-450), produced similar pozzolanic activity than that of SCBA C-650 with a SAI of 89.64%. In fact, no statistically significant difference was found between C-650 and P-450. Since post-processing of raw SCBA produces a significantly higher SCBA yield (i.e., 85 to 90) than that of controlled burning of SBF, post-processed SCBA P-450 was adopted for further investigation in concrete mixtures.

The effect of different dosages of post-processed SCBA P-450 (i.e., 20, 30, and 40% cement replacement by weight) on concrete properties was identified by evaluating the compressive strength (ASTM C39) at 28 and 90 days, slump (ASTM C143), surface resistivity (DOTD TR 233), water absorption (ASTM C642), and drying shrinkage (ASTM C157) on mixtures with target nominal compressive strengths of 27.6 MPa (4000 psi), i.e., Class-A, and 20.7 MPa (3000 psi), i.e., Class-B. For Class-A concrete mixtures, SCBA dosages of 10, 20, 30, and 40% of cement replacement by weight were evaluated. On the other hand, for Class-B concrete mixtures only a SCBA replacement of 20% was evaluated. In the case of Class-A concrete mixtures, increasing contents of SCBA produced a decrease in both the 28-day and 90-day compressive strengths. However, the 90-day surface resistivity and the relative strength gain from 28 to 90 days was significantly enhanced by the increments in SCBA content. Furthermore, it was determined that utilizing a 10% substitution of cement with post-processed SCBA produced a similar compressive strength to that of the control mixture after 90 days of curing (no statistically significant difference was encountered). In the case of Class-B concrete mixtures, a 20% cement replacement with SCBA produced a reduction in the compressive strength of concrete at 28 and 90 days of curing; yet, the difference between the 90-day compressive of control and the SCBA concrete was not

statistically significant. Furthermore, similarly to Class-A concrete mixtures, the 90-day surface resistivity and the relative strength gain from 28 to 90 days was significantly enhanced by the inclusion of SCBA. In terms of dimensional stability, an increase in drying shrinkage was observed for concrete mixtures containing SCBA. The increase in drying shrinkage were particularly noticeable at early stages of curing (i.e., 7, 14 days). Yet, after 28 days of curing increases in shrinkage were minor for SCBA mixtures compared to control. Finally, a cost analysis was performed to determine the feasibility of using SCBA as a concrete additive for pavement application. Results showed that the replacement of 10% of cement with SCBA in concrete could yield a reduction of per lane-mile cost of 0.75%.

1. INTRODUCTION

Bagasse is the fibrous by-product of sugarcane stalks after they are crushed to extract their juice. In 2016, the sugar production industry in Louisiana harvested 12,822,249 tons of sugarcane, which yielded 1,614,116 tons of sugar and almost 2,400,000 tons of bagasse *(1)*. Bagasse is used as a primary fuel source for sugar mills by burning the fibrous material into bagasse ash *(2)*. Based on the combustion procedure, the total production of bagasse ash is between 3% and 9% of the total dry fibrous bagasse production *(3)*. In the US, bagasse ash is currently considered an agricultural waste of no economic value that constitutes a fire hazard, with associated containment and disposal costs, as well as a potentially negative environmental impact (see Figure 1). Thus, the Louisiana sugar industry has a significant interest in finding a useful application of bagasse ash to minimize these disposal costs and reduce the fire hazard posed by fibrous bagasse.

Bagasse ash contains more than 50% by weight of silica (SiO_2), up to 10% by weight of lime (CaO), about 5% by weight of aluminum oxide (Al_2O_3), and several other chemical components in smaller amounts *(4)*. The high content of silica and aluminum oxide suggests that bagasse ash can exhibit pozzolanic behavior and be a suitable supplemental cementitious material (SCM) and substitute for cement in the production of concrete. In fact, when a pozzolanic material is added to cement, its amorphous silica reacts with the free lime released during the cement hydration and forms additional calcium silicate hydrate *(5)*. This phenomenon is well documented for rice husk ash *(6)*, which is known to improve the mechanical properties of concrete, e.g., its long-term compressive strength *(7)*.

(a) **(b)**

Figure 1. Land disposal of: (a) Bagasse ash and (b) Bagasse Fiber.

At the same time, the consumption of concrete in the US and particularly in Louisiana is steadily increasing, e.g., the consumption of cement went from 1.8M tons in 2002 to 2.2M tons in 2015 *(8)*. This consumption increase produces a significant need of new affordable and sustainable materials to be used as SCMs in concrete mixes. Bagasse ash could provide one alternative to reduce cement consumption and/or to substitute fine aggregates and/or fly ash. High-quality fly ash that satisfy ASTM C618 requirements *(9)* for use in concrete is relatively expensive ($50/ton) and produced at a lower level than the amount needed to keep up with the increase in concrete consumption in Louisiana and the US *(10)*. The use of pozzolanic additives as bagasse ash presents

several benefits *(11)*: (i) lower cost and lower carbon footprint of concrete, (ii) higher long-term compressive strength (e.g., at 90 days or more) at the expense of a small reduction of the 28-day compressive strength, and (iii) better durability.

2. OBJECTIVES

The aim of this study was to produce the necessary engineering knowledge to bring Sugar Cane Bagasse Ash (SCBA) closer to implementation as a Supplementary Cementitious Material (SCM) in the production of concrete for road pavement application by means of the following objectives:

- Develop an optimized production process to obtain bagasse ash with high pozzolanic activity;
- Determine the effects of bagasse ash on the mechanical and physical properties of concrete;
- Identify appropriate bagasse ash amounts to obtain concrete with properties that are compatible with its use for road pavement construction and repair.

3. LITERATURE REVIEW

3.1. Use of Bagasse in Cementitious Materials

Several researchers have studied the use of bagasse ash for concrete fabrication. Ganesan et al. *(12)* investigated the effects of bagasse ash content as a partial replacement of cement on relevant physical and mechanical properties of hardened concrete. The investigated properties of concrete included compressive strength, splitting tensile strength, water absorption, permeability characteristics, chloride diffusion, and resistance to chloride ion penetration. The experimental results reported in the study suggested that bagasse ash can be effectively used as a pozzolanic admixture with an optimal replacement ratio of cement equal to 20%. Montakarntiwong et al. *(13)* investigated the effects of loss on ignition (LOI, i.e., mass loss after prolonged heating), fineness, and cement replacement of bagasse ash on the compressive strength of concrete. Ordinary Portland cement was replaced by bagasse ash at levels of 20%, 30%, and 40% by weight of binder. Two levels of LOI (referred to as high and low LOI) and two levels of fineness (i.e., unground and ground) were considered in the study. The results revealed that the replacement of cement by ground bagasse ash with low and high LOI at 30% and 20% by weight of binder, respectively, resulted in a 28-day compressive strength as high as that of the control concrete. An important issue is the production process of the bagasse ash, and in particular the calcination temperature, which determines the portion of amorphous silica in the material and, thus, the reactivity of the bagasse ash with cement.

Modani and Vyawahare *(4)* investigated the effects of replacing the fine aggregate in concrete materials with untreated bagasse ash. In particular, fresh concrete tests (including compaction factor test and slump cone test) and hardened concrete tests (including compressive strength, split tensile strength, and sorptivity) were performed on concrete samples containing various amount of bagasse ash (i.e., 0%, 10%, 20%, 30%, and 40% by volume) as replacement of fine aggregate. The results of these experimental tests revealed that bagasse ash can be a suitable replacement of fine aggregate in concrete materials. In a similar study, Sua-iam and Makul *(14)* investigated the effects of replacing large amounts of fine aggregate by limestone powder and/or bagasse ash (i.e., 0%, 10%, 20%, 40%, 60%, 80%, or 100% by volume of only limestone powder, only bagasse ash, or an equal volume of limestone powder and bagasse ash). The results of this study showed that the replacement of fine aggregate by 20% limestone powder and 20% bagasse ash by volume effectively improved the workability and hardened properties of self-compacting concrete.

Amin evaluated the effects of replacing cement in concrete materials with raw SCBA (as received from the sugar mill). In particular, hardened concrete tests (including compressive strength, chloride diffusion, resistance to chloride ion penetration, and splitting tensile strength) were performed on concrete samples containing SCBA at seven different replacement levels, ranging from 0%-30% by mass (at increments of 5%) *(15)*. The study concluded that raw bagasse ash is a sustainable solution for cement replacement up to 20% by mass. Up to 20% cement replacement with SCBA, no significant reduction in compressive strength was reported. In addition, the partial replacement of cement with SCBA resulted in the development of high early strength and showed an improvement in resistance to chloride ion penetrability by 50% *(15)*.

Srinivasan and Sathiya studied the effects of raw SCBA (as received from the sugar mill) as a partial replacement of cement (at 0%, 5%, 10%, 15%, 20%, and 25% by mass) on relevant physical and mechanical properties of hardened concrete *(16)*. The investigated properties of fresh concrete

included compaction factor test and slump cone test. In the case of hardened concrete properties, compressive strength, flexural strength, split tensile strength, and modulus of elasticity were evaluated at 7 and 28 days. The study concluded that up to 10% cement replacement with SCBA had a significant impact on the properties of concrete producing higher compressive, flexural and tensile strength in comparison to that of control at 28 days. In addition, fresh concrete properties such as workability were also enhanced with the partial replacement of cement with SCBA. However, the density of concrete decreased with the increase in the SCBA content which is attributed to the lower density of SCBA compared to that of cement. The experimental results reported in the study suggested that SCBA can be effectively used as a pozzolanic admixture with an optimal replacement of cement of 10% by mass *(16)*.

3.2. Bagasse Ash Processing Methodologies

Cordeiro et al. characterized SCBA produced by the controlled burning the SBF at different temperatures (i.e., 400, 500, 600, 700 and 800°C) *(17*). The produced SCBAs were characterized by Energy Dispersive Spectroscopy (EDS), Scanning Electron Microscopy (SEM), specific surface area, and pozzolanic activity. The pozzolanic activity was determined by both Chapelle's method (chemical analysis) and strength activity index (SAI) method (mechanical method). The study concluded that SCBA produced by calcination at 350°C for 3 hours and then at 600°C for 3 additional hours presented the optimum combination of amorphous silica, low carbon content, high specific surface area, and considerable pozzolanic activity *(17)*. Furthermore, the study determined that utilizing calcination temperatures beyond 600°C, reduced the content of amorphous silica in SCBA.

In another study, Corderio et al. investigated the influence of SCBA particle size and surface area on its pozzolanic activity. In this study, different particle size distributions were obtained after grinding raw SCBA in the laboratory and in a pilot plant using different grinding mill types *(18)*. The grinded SCBA was then used as a partial replacement of cement at different levels (0%, 10%, 15%, and 20% by mass) to evaluate the relevant mechanical properties of hardened concrete. The study concluded that irrespective of the different particle size distributions obtained from different grinding configurations, the pozzolanic activity of SCBA was directly influenced by their fineness (characterized as their 80% passing size or Blaine specific surface area). Further, this study concluded that the pozzolanic activity of raw SCBA was significantly increased after grinding, i.e., it increased from 50% to 100% after grinding for prolonged times. Moreover, improved resistance to chloride ion penetration were reported at all levels of cement replacement in concrete with ultra-finely grinded SCBA *(18)*.

Hernandez et al. investigated the pozzolanic activity of bagasse ash obtained directly from the boilers of a sugar factory *(19)*. The study investigated the hydration reaction and properties of lime-SCBA binders by evaluating: (1) the pore structure by mercury intrusion porosimeter; (2) the calcium hydroxide content by XRD and Thermogravimetric Analysis (TGA); (3) the morphology utilizing SEM imaging; and (4) the compressive strength. The study concluded that high temperatures and incomplete combustion occurring in sugar factory boilers hinder the pozzolanic activity of SCBA by allowing the presence of impurities (i.e., unburned material and carbon) and formation of crystalline silica phases *(19)*.

Paya et al. compared the pozzolanic activity of SCBA directly obtained from the boilers of a sugar factory against SCBA produced under controlled conditions in the laboratory (i.e., burning at

600°C for 1 hour). The study concluded that SCBA obtained directly from the sugar mill is inadequate to be used as a SCM due to its high carbon and unburned material content, while SCBA produced under controlled laboratory conditions yielded an enhanced pozzolanic behavior due to lower carbon content and higher contents of the amorphous silica and alumina *(20)*. Bahurudden et al. compared the pozzolanic activity of raw SCBA (i.e., as obtained from the sugar mill) and post-processed SCBA (i.e., post-processed raw SCBA). The post-processed SCBA was produced from different methodologies including sieving, burning, grinding, and the combination of these *(21)*. The pozzolanic activity was assessed mechanically by strength activity index and chemically by Frattini's test. The study concluded that the calcination of raw SCBA at 700°C with subsequent grinding to cement fineness showed the optimum pozzolanic activity *(21)*. Furthermore, it was observed that burning SCBA at temperatures greater than 700°C produced crystallization of the silica; and therefore, a reduction in the pozzolanic activity *(21)*.

Govindarajan and Jayalaksmi characterized post-processed SCBA (produced by further burning of raw SCBA for 4 hours at different temperatures, ranging from 500°C to 1000°C in increments of 100°C). In this study, SCBAs were characterized using XRD and SEM techniques *(22)*. The study concluded that raw and post-processed SCBAs exhibit significantly different XRD patterns. The study reported the occurrence of a phase transformation at temperatures above 800°C associated with sharp and intense peaks on top of the amorphous background. This phenomenon was indicative of the crystallization of amorphous silica above 800°C. In addition, the study showed that post-processed SCBAs calcinated at 1000°C were highly crystallized and lacking of minor compounds such as calcium and iron oxides *(22)*. Furthermore, the study reported a change in color of post-processed SCBA particles from gray to white with the increase in temperature from 500°C to 1000°C. This change in color was attributed to the decrease in carbon content with the increase in temperature. Based on the experimental results, raw SCBA was not recommended to be utilized as a SCM due to its high carbon content. However, post-processed SCBA, which has significantly less carbon content, can be used as a SCM *(22)*.

In another study, Govindarajan and Jayalakshmi studied the influence of post-processed SCBA as a partial replacement of cement on the properties of cement mortar *(23)*. In this study, the post-processed SCBA was produced by burning raw SCBA at 600°C for 4 hours in laboratory conditions and grinding (such that the SCBA passes through a 75μm sieve). The properties of cement pastes containing post-processed SCBA at cement replacements of 5%, 10%, 15%, and 20% (by mass) were characterized by compressive strength test, X-ray Diffraction, and Fourier-Transform infrared spectroscopy (FTIR) *(23)*. The study concluded that mortars containing post-processed SCBA, at all cement replacement levels, resulted in higher compressive strength than that of control mortars (at 1, 7, and 28 days). The increase in compressive strength was attributed to the filler and the pozzolanic effect of SCBA. However, the compressive strength of mixtures with 15% and 20% cement replacement with SCBA were lower than the mixtures with 5% and 10% replacement (attributed to a dilution effect). The study reported maximum increase in compressive strength at 10% and recommended this as an optimum level for the replacement of cement with SCBA. In the case of the XRD analysis, diffraction peaks for $Ca(OH)_2$, ettringite, and C-S-H phase were observed in all mortars samples (which were formed during the hydration process). Furthermore, the study also reported a reduction of $Ca(OH)_2$ and an increase in C–S–H on cement pastes containing post-processed SCBA, which is indicative of the reaction between $Ca(OH)_2$ and the amorphous silica present in post-processed SCBA.

4. METHODOLOGY

4.1. Materials

In this study, the utilized SBF and raw SCBA materials were collected from Alma Plantation, which is a Louisiana based sugar factory. Both SBF and SCBA were randomly collected from a stockpile, as presented in Figure 1. The collected materials were used to investigate the properties of SCBA produced from 3 different production methodologies, i.e., raw SCBA, controlled SCBA and post-processed SCBA. The different production methodologies are explained in detail in following sub-sections.

4.1.1. Raw SCBA

Raw SCBA was the bagasse ash directly collected from the sugar mill which is produced from the uncontrolled burning of SBF (Figure 2a) in a sugar factory. In this study, raw SCBA was minimally processed by drying at 65°C for 24 hours and, subsequently, sieving using a No. 20 (841 μm) sieve. Drying was performed to remove moisture while sieving was performed to remove coarse impurities (i.e., unburnt fibers, gravel, etc.). The sieved SCBA was then grinded at 300 rpm in a jar mill for 35 minutes. The raw SCBA material obtained after drying, sieving and grinding was designated as BA-U (Figure 2b).

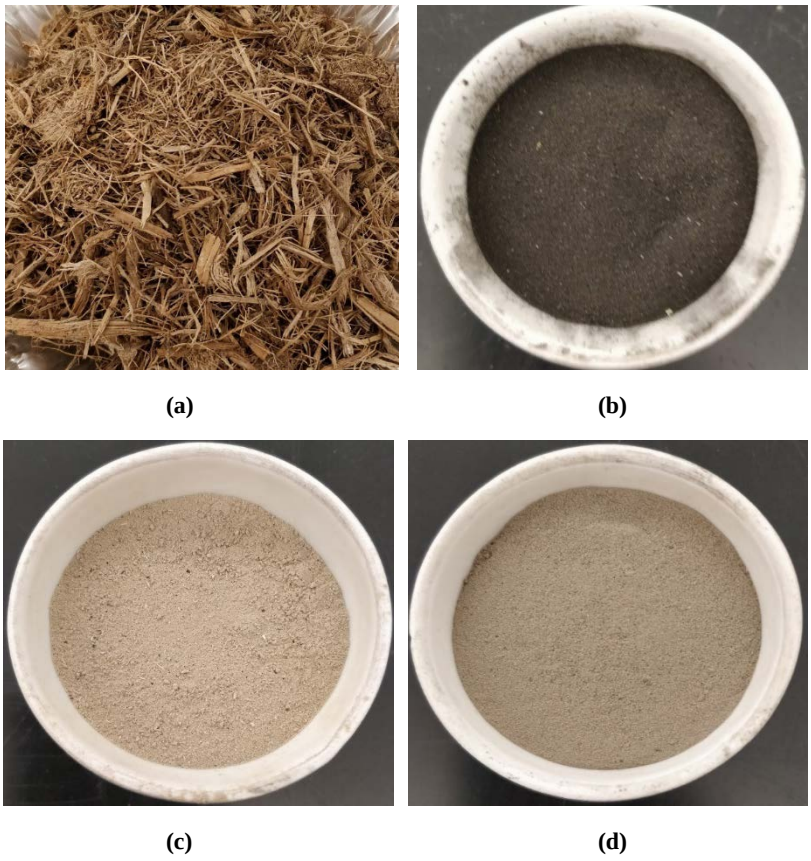

Figure 2. Bagasse samples: (a) SBF (b) BA-U (c) C-550 and (d) P-550.

4.1.2. Controlled SCBA

The bagasse ash labeled as controlled SCBA was the SCBA produced by the controlled burning of SBF in the laboratory (as shown in Figure 2c). The SBF collected from the sugar mill was washed with water to remove impurities and then allowed to air dry. The dry SBF was initially burned at 350°C for 1 hour in a muffle furnace. In order to obtain a homogeneous sample, all batches of bagasse ash obtained from the initial burning SBF were combined. Subsequently, the bagasse ash was divided into equal parts by using a splitter. Next, each of the parts was burned for two additional hours at 350°C, and, then burned for another 3 hours at different temperatures from 450°C to 650°C (at increments of 50°C). After completion of the calcination process, all samples were allowed to cool inside the furnace until the temperature dropped to 80°C. Furthermore, the controlled SCBA materials were grinded in the same way as raw SCBA (in a jar mill at 300 rpm for 35 minutes). In total, five different controlled SCBA materials (i.e., burned at 5 different temperatures), were produced from this methodology. As presented in Table 1, the controlled SCBA materials were designated as C-T, where T represents the highest calcination temperature.

Table 1. Bagasse ash produced from different methodology.

Production Methodology	Calcination Temperature (°C)	ID	Tests Performed (No. of Replicas)
Raw SCBA (Uncontrolled)	-	BA-U	SEM (1) EDS (3) XRD (1) Particle Size Analysis (1) Strength Activity Index (6)
Controlled SCBA	450	C-450	
	500	C-500	
	550	C-550	
	600	C-600	
	650	C-650	
Post-processed SCBA	450	P-450	
	500	P-500	
	550	P-550	
	600	P-600	
	650	P-650	

4.1.3. Post-Processed SCBA

The material labeled as post-processed SCBA was the bagasse ash obtained by the post-processing of raw SCBA (as shown in Figure 2d). After drying and sieving (according to section 4.1.1 guidelines), raw SCBA was further processed by burning and grinding under controlled laboratory conditions. The burning process consisted of 2 hours at 350°C and then 3 hours at different sets of temperature ranging from 450°C to 650°C (at increments of 50°C). The burning temperatures utilized for post-processing were the same as the ones utilized for calcination of controlled SCBA. After completion of the calcination process, the materials were allowed to cool inside the oven until the temperature reached 80°C. All post-processed SCBAs were grinded following the same procedure utilized for raw and controlled SCBAs. The post-processed SCBA materials were designated as P-T where T represents the highest calcination temperature.

4.1.4. Cement

Ordinary Portland Cement Type I conforming to ASTM C150 standard, was used in the study *(24)*. The chemical composition of the cement is presented in Table 2. The specific gravity of the cement was 3.15.

Table 2. Cement Chemical Composition (by weight).

SiO_2	Al_2O_3	Fe_2O_3	CaO	Na_2O	K_2O	SO_3	MgO
19.80	4.70	3.80	64.80	0.16	0.54	3.38	2.20

4.1.5. Aggregates

For the concrete mixtures produced in this study, the coarse aggregate utilized was limestone with a specific gravity of 2.7 and maximum aggregate size of 19-mm (0.75-in). Furthermore, the fine aggregate utilized for concrete mixtures was silica sand with a specific gravity of 2.67 and a fineness modulus of 2.61. Standard graded sand conforming to ASTM C778 *(25)* was used for the Strength Activity Index evaluation.

4.1.6. Superplasticizer

A polycarboxylate based High-Range Water Reducer (HRWR), was utilized in this study for all concrete mixtures produced. A dosage of 0.38 % by weight of binder was used in all concrete mixtures.

4.2. Bagasse Ash Characterization

In order to determine an optimum production methodology to maximize the pozzolanic activity of SCBA, the physical and chemical properties of the 11 different types of SCBA materials produced were thoroughly investigated. The different analysis conducted are described in the following sub-sections.

4.2.1. Microstructure and Chemical Composition

The properties of concrete containing SCMs are significantly influenced by the chemical composition, shape, and particle size of the SCMs. Hence, the morphology (shape and size) of bagasse ash was investigated from Scanning Electron Microscopy (SEM), and the chemical composition was determined from Energy Dispersive X-Ray Spectroscopy (EDS) and X-ray Fluorescence (XRF). The scanning electron microscope used in this study, as illustrated in Figure 3, was the Quanta™ 3D Dual Beam™ FEG FIB-SEM, with EDAX Pegasus EDS/EBSD detectors. In addition to the EDS, the PANalytical Epsilon 3XLE EDS X-ray Fluorescence Spectroscopy system was used. This analysis was performed to ensure that the ASTM C618 chemical composition requirements were met.

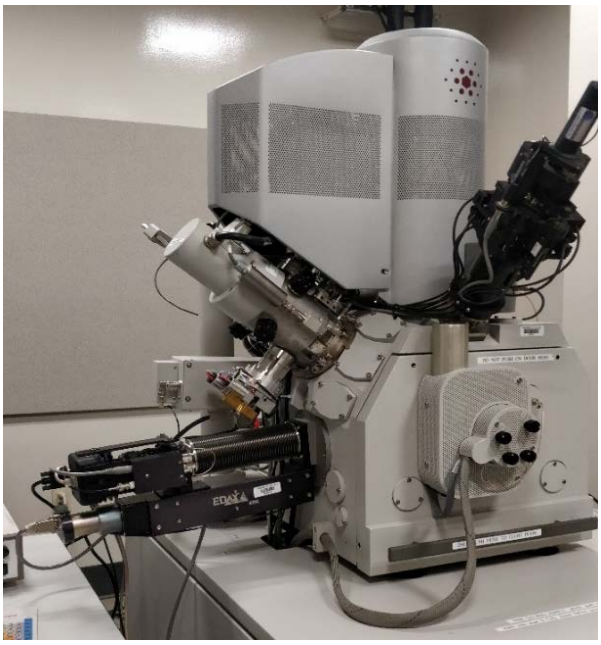

Figure 3. Quanta™ 3D DualBeam™ FEG FIB-SEM for SEM-EDS.

4.2.2. X-Ray Diffraction (XRD)

The pozzolanic activity of bagasse ash is significantly influenced by the amorphous silica content in the material. Hence, a mineralogical analysis was conducted on a powder sample by using Panalytical Empyrean X-ray Diffractometer. The equipment utilized in this study is presented in Figure 4. The X-ray diffraction technique was carried out using Cukα radiation at 40mA and 45kV. The intensity for each specimen was determined by a scan step size of 0.026° in the range of 10°-80° 2θ. The crystalline phases in bagasse ash were identified by comparing the standard quartz 50-50 powder.

Figure 4. Panalytical Empyrean X-ray Diffractometer for XRD analysis.

4.2.3. Grinding and Particle Size Analysis

In order to reduce the particle size of SCBA materials and increase its pozzolanic activity, grinding was conducted utilizing a U.S. Stoneware 784 CV jar rolling mill (as shown in Figure 5) at 300 rpm for 35 minutes.

Figure 5. Jar mill grinding.

The particle size distributions of SCBAs before and after grinding were analyzed using a Beckman Coulter LS200 laser diffraction analyzer (as shown in Figure 6). The laser diffraction analyzer utilized had the capability of detecting particles between 0.4 µm to 2000 µm *(26)*. The particle size distributions were assessed using a micro-volume module. Samples were suspended in water with agitation and a run time of 60 seconds.

Figure 6. Beckman Coulter LS 200 for Particle size analysis.

4.2.4. Moisture Content and Loss on Ignition

The moisture content and LOI were determined according to ASTM C311. For moisture content determination, 1 g of SCBA material was weighed in a porcelain crucible and kept inside the furnace at 110°±5°C until constant mass was achieved. Subsequently, the samples were taken out of the oven and allowed to cool inside a desiccator. Finally, the samples were weighed, and the moisture content was calculated using Equation 1. For LOI determination, the dried and cooled

sample utilized for moisture content evaluation was ignited at 750°C for 45 minutes and then allowed to cool at the room temperature inside a desiccator. The cooled sample was weighed and LOI was calculated using Equation 2 *(27)*.

$$Moisture\ Content, \% = \frac{X}{Y}\ X\ 100 \quad [1]$$

where:
X= mass loss due to drying; and
Y= initial mass.

$$Loss\ on\ Ignition, \% = \frac{B-C}{B-A}\ X\ 100 \quad [2]$$

where:
A = mass of empty crucible;
B = mass of dried sample and crucible from moisture content; and
C = mass of ignited sample and crucible.

4.2.5. pH Evaluation

The pH of SCBA was evaluated in order to gain insight on the alkalinity of SCBA; and therefore, on its compatibility with the cement hydration reaction. The pH of bagasse ash was measured per ASTM D5239. According to the standard, 20g of SCBA were added to 80mL of distilled water and were stirred to disperse the bagasse ash. The mixture was left undisturbed for 2 hours and subsequently the pH was determined by using a pH meter *(28)*. The pH meter calibration was performed in accordance with test method ASTM D1293 *(29)*. It should be noted that pH evaluation was only performed on the bagasse ash that yielded the maximum pozzolanic activity.

4.2.6. Total Water-Soluble Sulfates

High amounts of SO_3 can increase drying shrinkage of concrete and increases the risk of delayed ettringite formation *(30)*; thus, its content is limited in ASTM C618 standard. Complementary to the EDS results, the SO_3 content was determined per ASTM D5239. According to the standard, 1 g of bagasse ash was stirred in 100 mL of distilled water for 2 min and subsequently filtered *(28)*. At the end of the filtration process, a 50 mL aliquot of filtrate was separated and diluted to 250 mL by adding distilled water. Next, 5 mL of concentrated hydrochloric acid (HCl) were added to the 250 mL solution and mixed vigorously. Subsequently, 10 mL of Barium chloride ($BaCl_2$) were added to the acid solution and then boiled until a sulfate precipitate was formed. The solution was digested for 24 hours at a temperature just below boiling point and the volume of the solution was maintained between 225-260mL *(31)*. At the end of the digestion period, the solution was filtered and the residue was ignited at 800°C for 30 minutes. After ignition of the residue, the sample was allowed to cool inside a desiccator and subsequently weighed. The percentage of SO_3 was calculated using Equation 3.

$$SO_3, \% = W\ X\ 34.3 \quad [3]$$

where:
W = residue after ignition (grams of $BaSO_4$); and
34.3 = molecular ratio of SO_3:$BaSO_4$ (0.343) X 100.

4.2.7. Strength Activity Index

The pozzolanic activity of all SCBA materials was evaluated by utilizing the Strength Activity Index (SAI) method according to ASTM C311 *(27)*. The control mixture was labeled as CO and was prepared according to the standard by mixing 500 g of Portland cement, 1375 g of standard graded sand conforming to ASTM C778 *(25)*, and 242 mL of water. Subsequently, the mixture was casted into six control mortar cubes 50.8-mm (2-in) inside. The flow value of the control mixture was determined per ASTM C1437 *(32)*. Similarly, mortars containing a 20% cement replacement by weight with SCBA were prepared and cast for each SCBA material produced in this study. For mixes with SCBA, the amount of water required was determined such that the same flow value as that of the control mixture was achieved (within ±5% tolerance). After 24 hours, the cubes were demolded and cured in a 23 ± 2°C, >95% Relative Humidity (RH) room, according to ASTM C192 *(33)*. At 28 days of curing, the compressive strength of mortars was measured following ASTM C109 standard *(34)*. The test setup is presented in Figure 7. The strength activity index was calculated using Equation 4.

$$SAI = \frac{A}{B} * 100 \qquad [4]$$

where:
A = average compressive strength of SCBA mixture cubes; and
B = average compressive strength of control mixture cubes.

It should be noted that, per ASTM C618 *(27)*, a minimum SAI of 75% is required for a material to qualify as a SCM.

Figure 7. Compressive strength testing setup for 50.8-mm (2-in) mortar cubes.

4.3. Testing of Bagasse Ash Admixed Concrete

The initial phase of this study focused on the characterization of SCBA materials to determine its suitability as SCMs. In this subsequent phase, the properties of concrete admixed with SCBA are evaluated on mixtures with target nominal compressive strengths of 20.7 MPa (3000 psi) (concrete for underdrain systems and concrete sidewalks) and 27.6 MPa (4000 psi) (concrete for road pavements). Mechanical and physical properties of concrete with 10%, 20%, 30% and 40% cement replacement (by weight) with SCBA were experimentally investigated. Properties evaluated included compressive strength, surface resistivity, drying shrinkage, slump, and water absorption.

4.3.1. Mix Proportioning

A total of seven different concrete mixtures were prepared to evaluate the impact of bagasse ash dosage on the properties of concrete. Two types of concretes were produced, 27.6 MPa (4000 psi) and 20.7 MPa (3000 psi) target compressive strength concretes labeled as Class-A and Class-B concretes, respectively. Control concrete mixtures (without bagasse ash) were designated as CO-4 and CO-3, for Class-A and Class-B concrete, respectively. Similarly, concrete mixtures containing bagasse ash were designated as P-4-X and P-3-X, for Class-A and Class-B concretes, respectively, where X represents the weight % of cement replaced with bagasse ash. The percentages of cement replacement (by weight) evaluated were 10%, 20%, 30% and 40% for Class-A mixtures and 20% Class-B mixtures. The binder content, slump range and water to binder ratio were selected per LaDOTD specification *(35)*. All the mixtures were prepared with a water to binder ratio (W/(C+SCBA)) of 0.48. The binder content for Class-A mixtures was 296.6 kg/m^3, while the binder content for Class-B mixtures was 287.7 kg/m^3. The mix proportions for all seven concrete mixtures are summarized in Table 3.

Table 3. Concrete mixture proportions.

ID	Target Compressive Strength (psi)	SCBA (%)	Index	Cement (kg/m^3)	Bagasse Ash (kg/m^3)	Coarse Aggregate (kg/m^3)	Fine Aggregate (kg/m^3)	Water (kg/m^3)
Class-A	27.6 (4000)	0	CO-4	296.6	-	1159.1	758.2	142.4
		10	P-4-10	266.9	29.7	1154.8	755.4	142.4
		20	P-4-20	237.3	59.3	1150.5	752.5	142.4
		30	P-4-30	207.6	89.0	1146.2	749.7	142.4
		40	P-4-40	178.0	118.6	1141.9	746.9	142.4
Class-B	20.7 (3000)	0	CO-3	287.7	-	1170.6	765.7	138.1
		20	P-3-20	230.2	57.5	1162.3	760.3	138.1

4.3.2. Specimen Preparation

Concrete mixtures were prepared utilizing a drum mixer. Initially, coarse aggregates and 2/3 of the mixing water were introduced into the drum and mixed for 3 minutes. Subsequently, all the remaining components and water were added to the drum and mixed for 3 additional minutes. Next, the mixture was allowed to rest for 3 minutes followed by 3 additional minutes of mixing. After the mixing process was completed, the slump of fresh concrete was determined. Subsequently, six cylindrical specimens and three prismatic specimens (for shrinkage evaluation) were casted per each concrete mixture. After 24 hours, cylindrical specimens were demolded and allowed to cure in a moist room (23 ± 2°C, > 95% Relative Humidity [RH]) according to ASTM C192 *(33)*. In the case of the prismatic specimens for shrinkage determination, specimens were demolded and cured in lime saturated water following ASTM C157 standard *(36)*.

4.3.3. Compressive Strength Test

After 28 and 90 days of curing, the compressive strength of the different concrete materials produced was evaluated according to ASTM C39 on 101.6-mm x 203.2- mm (4-in x 8-in) cylinders *(37)*. For each curing age, three replicas were evaluated. The test setup for compressive strength

testing is presented in Figure 8. The compressive strength tests were performed under hydraulic pressure with a constant loading rate of 0.25 MPa/s.

Figure 8. Compression test setup.

4.3.4. Surface Resistivity

The permeability of concrete is one of the most important properties influencing its durability. A permeable concrete can allow for the ingress of deleterious substances into the material such as chloride ion. In turn, this can significantly enhance the deterioration of a concrete structure. In this study, chloride ion penetrability of concrete mixtures was investigated by DOTD TR233 "Test Method for Surface Resistivity Indication of Concrete's Ability to Resist Chloride Ion Penetration" *(38)*. This test evaluates the electrical resistivity of concrete and provides an indicator of concrete chloride ion penetration. According to the surface resistivity test, the higher the electrical resistivity of concrete, the lower the probability of chloride ion penetration should be. Since the surface resistivity test is non-destructive, the test specimen evaluated were the same concrete cylinders utilized for compressive strength determination. A Proceq Resipod surface resistivity meter (with a 1.5" probe spacing) was used to measure the electrical resistivity of the concrete cylinders. After the cylinders were removed from the curing chamber, the electrical resistivity readings were taken at the center of the longitudinal axis of the cylinders at 0°, 90°, 180°, and 270°. Initially, a random location was assigned as 0°, subsequently the cylinder was rotated counterclockwise to the remaining testing locations. For each specimen, 2 sets of reading were taken at each location (i.e., 0°, 90°, 180°, and 270°) as shown in Figure 9. The average resistivity for each set was multiplied by the curing factor (1.1 for lime water curing and 1 for moist room curing), which in our case was 1.

Figure 9. Surface resistivity setup.

The qualitative chloride-ion penetrability equivalent to the measured surface resistivity was reported for each concrete mixture based on values presented in Table 4.

Table 4. Chloride Ion Penetrability Based.

Chloride Ion Penetrability	4 in. X 8 in. Cylinder (KOhm-cm), a=1.5"*	6 in. X 12 in. Cylinder (KOhm-cm), a=1.5"*
High	<12.0	<9.5
Moderate	12.0-21.0	9.5-16.5
Low	21.0-37.0	16.5-29.0
Very Low	37.0-254.0	29.0-199.0
Negligible	>254.0	>199

*Note: a= Wenner probe spacing

4.3.5. Drying Shrinkage

Drying shrinkage is a crucial property for concrete materials used in road pavement rehabilitation. Excessive shrinkage can produce delamination and early cracking, thus, causing premature deterioration of the repair system. In this study, drying shrinkage was assessed by measuring the length change of a concrete prismatic specimen following ASTM C157 standard. The test specimens utilized had a 75-mm (3-in) square cross-section and were 254-mm [10-in] in length *(36)*. The test specimens were casted in accordance with ASTM C192 and demolded after 24 hours. Right after demolding, specimens were immersed in lime saturated water at 23 ± 2°C according to ASTM C157. After 30 minutes, the initial reading was taken as shown in Figure 9. Subsequently, the specimen was immersed again in the lime saturated water container. At 28 days of curing, a second reading was taken. The length change of each specimen was calculated using Equation 5 *(36)*.

$$\Delta L_x = \frac{CRD - initial\ CRD}{G}\ X\ 100 \qquad [5]$$

where:

ΔL_x= Length change of any specimen at any given age %;

CRD = Difference between the comparator reading of the reference bar and the specimen at any given age; and
G = Gage length (250-mm [10 inch]).

Figure 10. Comparator dial reading setup with test specimen.

4.3.6. Water Absorption

In this study, the water absorption of concrete specimens was determined following ASTM C642 standard. This test method estimates the water permeable pore space in hardened concrete by measuring the maximum amount of water absorbed by a dry concrete specimen. Initially, a portion of a cylinder (free from cracks) was weighed and dried in an oven at a temperature of 110 $\pm$5°C for 24 hours *(39)*. After 24 hours the specimen was taken out of the oven and allowed to cool at room temperature. The mass of the dry specimen was determined and then the specimen was immersed in water (at approximately 21°C) for 48 hours or until the successive weight readings at an interval of 24 hours showed an increase of no more than 0.5%. After this was achieved, the final weight was recorded and the water absorption was calculated utilizing Equation 6 *(39)*.

$$\text{Absorption after immersion, \%} = \frac{B-A}{A} X\ 100 \qquad [6]$$

where:
A= mass of oven dried sample in air; and
B= mass of surface-dry sample in air after immersion.

5. ANALYSIS AND FINDINGS

5.1. Bagasse Ash Microstructure Characterization and Pozzolanic Activity

5.1.1. Microstructure and Chemical Composition

The morphology of all SCBA materials produced in this study were investigated by SEM imaging. Figure 11 provides morphological information of the different phases observed in raw SCBA. It should be noted that raw bagasse ash was produced from the uncontrolled burning of SBF. Hence, as shown in Figure 11, raw SCBA consists of a combination of fiber (i.e., elongated and coarse fibrous particles) and ash (i.e., fine irregular and prismatic particles) particles. The observation of fibers-like features in raw SCBA occurred likely due to the large temperature gradients occurring during uncontrolled burning of SBF which allow for portions of SBF to remain unburned. From SEM imaging, prismatic particles were clearly observed as indicated in Figure 11. The presence of prismatic particles was attributed to the presence of crystallized silica due to high calcination temperatures *(21)*. Even though bagasse is typically burnt at 500°C to 600°C in the sugar mills, particles present near the furnace funnel opening can experience higher temperatures producing crystallization of the amorphous silica *(21)*. Furthermore, irregular particles observed in Figure 11 were likely amorphous silica.

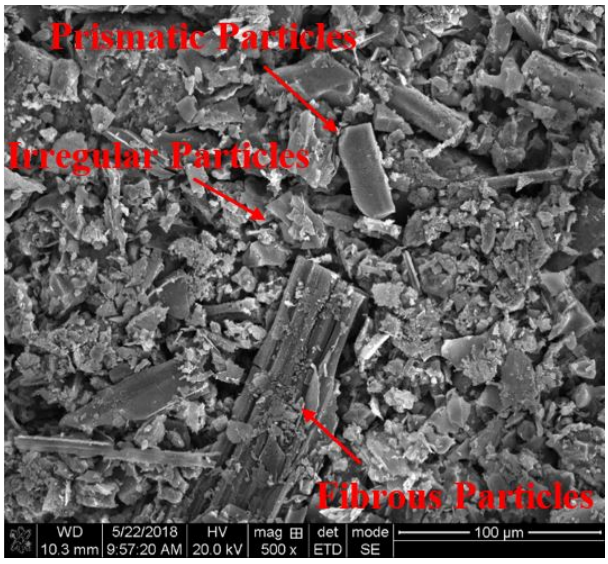

Figure 11. SEM image of raw bagasse ash at 500X magnification.

The microstructure of controlled SCBAs after being processed at different calcination temperatures are presented in Figure 12. Since controlled SCBAs were produced by burning SBF under controlled laboratory conditions (i.e., small temperature gradients), the materials were mostly free from fibrous and prismatic particles. Furthermore, the size of the particles in controlled SCBAs were much smaller than those observed in raw SCBA; yet, particles with irregular shapes and different sizes were observed. From the SEM images presented in Figure 12, it is important to notice that similar particle morphology (size and shape) was observed in controlled SCBA materials produced at the different calcination temperatures investigated in this study.

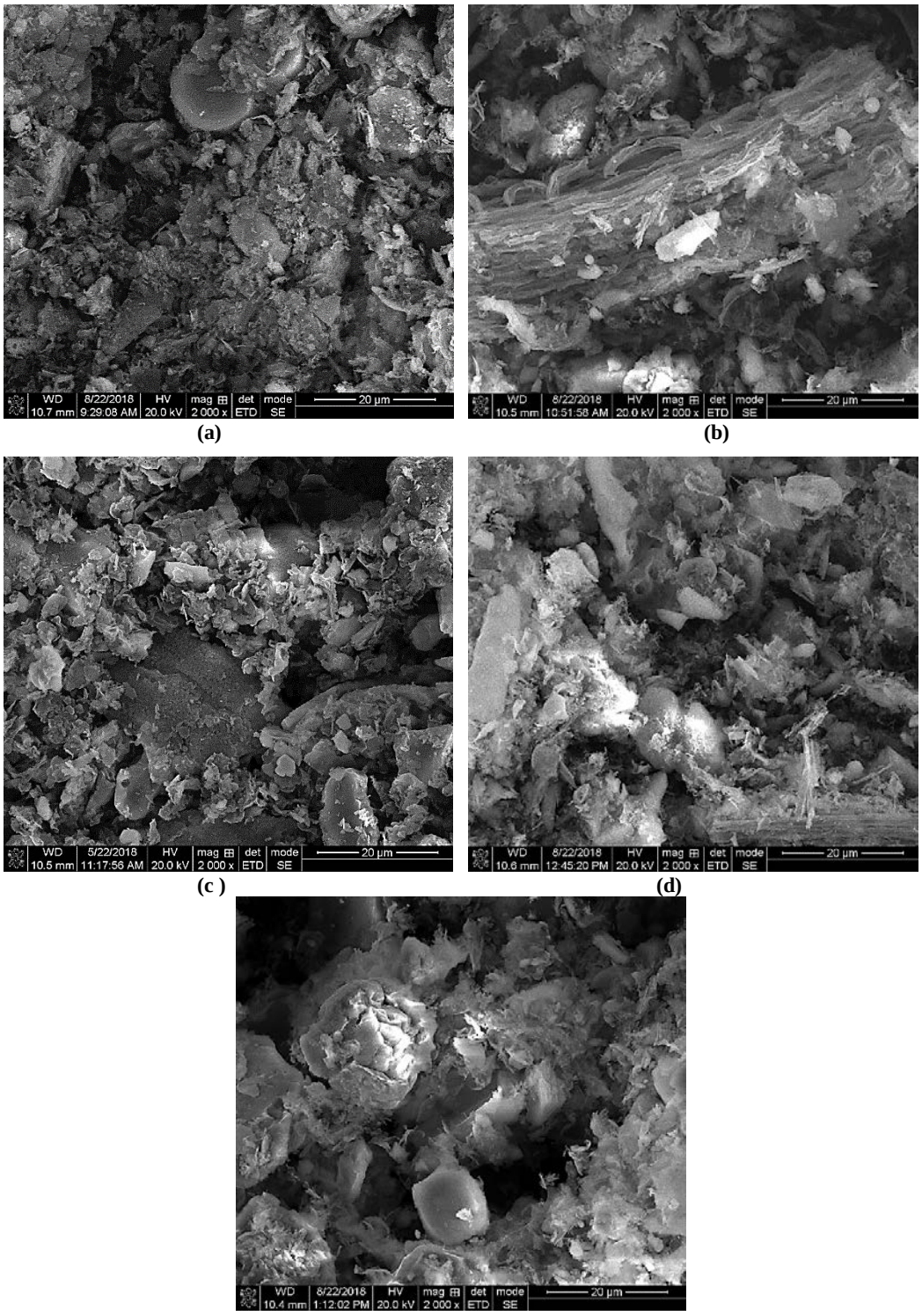

(a) **(b)**

(c) **(d)**

(e)

Figure 12. SEM images for: (a) C-450, (b) C-500 (c) C-550 (D) C-600 and (e) C-650.

Figure 13 presents SEM images of post-processed SCBA materials burned at different temperatures. As shown in Figure 13, no fiber-like features were observed. Furthermore, particles were mostly small and irregular in shape. Since post-processing consist of further burning of raw SCBA, it was expected that residual fiber particles observed in raw SCBA would be consumed during post-processing; thus, absent in post-processed SCBA materials. In addition, prismatic particles (attributed to the presence of crystalized silica) and irregular particles (attributed to the presence of amorphous silica) were observed for post-processed SCBA. Moreover, it was observed that post-processed SCBA particles were similar to those observed in controlled SCBA materials.

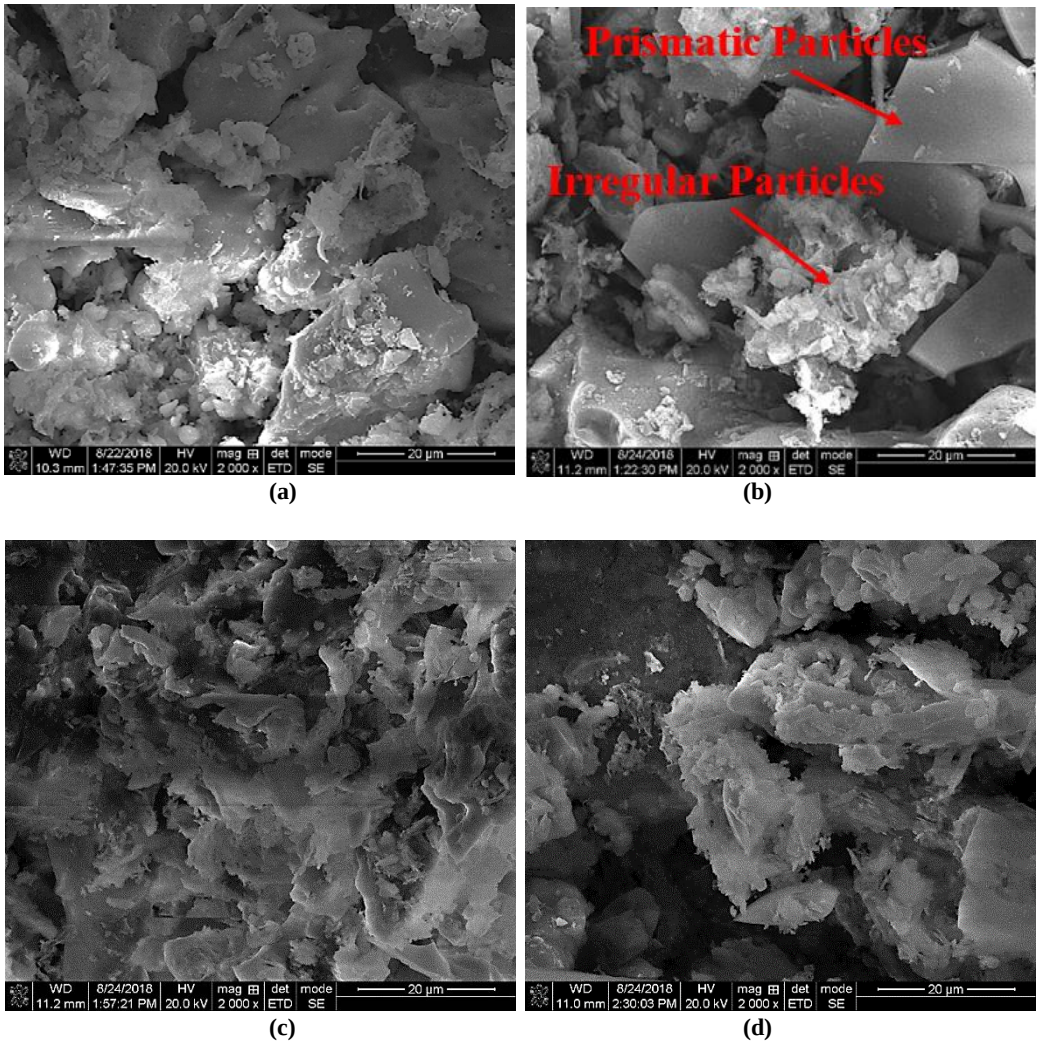

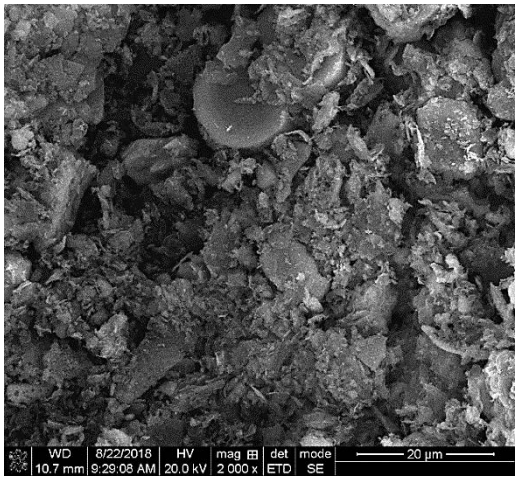

(e)

Figure 13. SEM images for: (a) P-450, (b) P-500 (c) P-550 (D) P-600 and (e) P-650.

EDS spectra were collected utilizing area mode to determine the chemical and oxide composition of the different SCBAs considered in this study. EDS spectra were collected with an accelerating voltage of 20kV and a current of 4pA. Both, oxide and elemental composition, were determined and presented in Tables 5 and 6, respectively. Excepting raw SCBA, the pozzolanic component (i.e., SiO_2+Al_2O_3+Fe_2O_3) in all the SCBA materials was greater than 70%; thus, meeting the minimum pozzolanic content requirement per ASTM C618 (i.e., 70% for Class N and F fly ash, and 50% for Class C fly ash) *(9)*. It is important to notice that raw SCBA failed to meet the ASTM C618 pozzolanic component requirement due to high carbon content as shown in Tables 5 and 6. It should be noted that CO_2 content was not included in the oxide composition of both controlled and post-processed SCBAs due to a high error associated with the CO_2 estimation (due to very low carbon content). Furthermore, the EDS analysis results showed that the amount of SO_3 in all the SCBA materials was much lower than the maximum allowable limit per ASTM C618 (i.e., 4% for class N fly ash and 5% for class F and C fly ash) *(9)*.

Along with the EDS, XRF analysis was conducted to determine chemical composition of SCBA materials. For XRF analysis, SCBA powdered samples (0.6 g) were fused with a mix of Li-tetraborate, Li-metaborate and Li-iodide (total mass of 6 g) in a Clarisse LENeo fluxer at 1100°C to glass beads. The chemical composition obtained from XRF analysis is presented in Table 5b. From EDS analysis, it was observed that carbon was the main constituent in raw SCBA; yet, XRF result shows absence of carbon in raw SCBA. This is the case since the XRF equipment is not capable of detecting elements lighter than magnesium; thus, the presence of carbon in raw SCBA was not detected. Furthermore, for all controlled and post-processed SCBAs, the sum of the pozzolanic component obtained from XRF were higher than the values reported from EDS analysis. It is also important to note that XRF reported minor differences in the pozzolanic component between each of the controlled and post-processed SCBA materials. Due to the aforementioned limitation of XRF (i.e., carbon cannot be detected), for comparative purposes within the different SCBA materials, EDS results will be referred to throughout this report.

Among all the SCBAs considered in this study, C-650 and P-450 showed the highest amount of pozzolanic component of 86.13% and 85.97%, respectively, in EDS analysis. It is important to notice that the difference in pozzolanic component between C-650 and P-450 were almost negligible with C-650 outperforming P-450 by only 0.16%.

Table 5. SCBA oxide composition (by weight) (a) EDS Analysis (b) XRF

(a)

Oxide	BA-U	C-450	C-500	C-550	C-600	C-650	P-450	P-500	P-550	P-600	P-650
CO_2	66.15	-	-	-	-	-	-	-	-	-	-
Na_2O	0.30	2.97	3.23	2.70	2.63	2.43	0.67	0.73	0.73	1.50	1.33
MgO	0.45	2.03	2.07	1.67	1.87	1.47	1.23	2.53	2.53	2.20	2.10
Al_2O_3	2.65	9.50	9.13	7.93	8.20	7.83	7.40	7.50	7.50	11.00	10.57
SiO_2	22.95	66.10	65.87	70.10	68.63	74.03	73.53	69.67	69.67	64.17	62.90
P_2O_5	3.00	5.20	5.07	2.23	3.00	1.13	2.37	2.27	2.27	2.10	3.53
SO_3	0.00	1.43	1.47	0.97	1.23	0.63	0.33	0.47	0.47	0.50	0.70
K_2O	1.50	4.37	4.27	4.27	3.97	3.77	4.70	4.63	4.63	5.13	5.70
CaO	1.55	4.50	4.80	5.17	4.60	4.40	4.73	7.73	7.73	5.20	6.33
Fe_2O_3	1.60	3.90	4.10	5.00	3.77	4.27	5.03	4.50	4.50	8.23	6.87
Pozzolanic Component (SiO_2+Al_2O_3+Fe_2O_3)	27.20	79.50	79.10	83.03	80.60	86.13	85.97	81.67	81.67	83.40	80.33

(b)

Oxide	BA-U	C-450	C-500	C-550	C-600	C-650	P-450	P-500	P-550	P-600	P-650
Na_2O	0.73	1.59	1.72	1.72	1.68	0.79	0.72	0.78	0.93	0.81	0.79
MgO	1.25	1.18	1.05	1.05	1.11	1.28	1.23	1.28	1.29	1.30	1.28
Al_2O_3	7.65	7.26	7.61	7.61	7.61	7.67	7.55	7.68	7.67	7.69	7.67
SiO_2	78.58	76.98	79.94	79.95	80.00	78.45	78.52	78.55	78.30	78.44	78.46
P_2O_5	0.94	0.68	0.70	0.70	0.71	0.93	0.92	0.93	0.92	0.92	0.93
SO_3	0.00	0.50	0.50	0.50	0.54	0.53	0.45	0.56	0.50	0.50	0.53
K_2O	4.46	2.87	2.96	2.96	2.95	4.45	4.45	4.42	4.46	4.44	4.45
CaO	3.07	5.84	2.39	2.40	2.31	3.01	3.03	3.00	3.01	2.99	3.01
TiO_2	0.39	0.37	0.39	0.39	0.39	0.39	0.39	0.38	0.39	0.38	0.39
Fe_2O_3	2.53	2.23	2.24	2.24	2.21	2.53	2.65	2.50	2.50	2.50	2.52
I	0.11	0.20	0.20	0.19	0.20	0.16	0.18	0.10	0.18	0.17	0.16
Pozzolanic Component (SiO_2+Al_2O_3+Fe_2O_3)	88.75	86.47	89.79	89.81	89.82	88.64	88.71	88.73	88.47	88.63	88.65

Table 6. SCBA elemental composition (by weight).

Element	BA-U	C-450	C-500	C-550	C-600	C-650	P-450	P-500	P-550	P-600	P-650
C	40.05	-	-	-	-	-	-	-	-	-	-
O	30.20	42.33	42.20	44.30	41.96	45.97	46.43	46.13	44.30	44.20	43.43
Na	0.10	2.37	2.57	2.13	2.19	1.93	0.67	0.67	2.13	2.19	1.13
Mg	0.30	1.37	1.40	1.10	1.25	1.00	1.67	1.67	1.10	1.25	1.40
Al	2.15	5.57	5.37	4.50	4.97	4.43	4.20	4.20	4.50	4.97	5.97
Si	18.10	34.60	34.47	35.13	36.97	36.37	33.53	33.53	35.13	36.97	31.47
P	2.5	2.50	2.47	0.97	1.51	0.43	0.90	0.90	0.97	1.51	1.57
S	0.00	0.53	0.57	0.37	0.47	0.23	0.10	0.10	0.37	0.47	0.23
K	2.25	3.97	3.87	3.73	3.72	3.23	3.90	3.90	3.73	3.72	4.93
Ca	2.10	3.60	3.90	3.97	3.88	3.33	5.57	5.57	3.97	3.88	4.83
Fe	2.15	3.07	3.20	3.73	3.07	3.13	3.27	3.27	3.73	3.07	5.13

5.1.2. X-ray Diffraction (XRD)

XRD analysis was performed by using the Highscore v4.7 software based on a Rietveld method. Since most SCBAs exhibited very similar XRD patterns, only C-450, P-450 and BA-U are presented in Figure 14. The patterns observed in Figure 14 included an amorphous bump between 2θ angles of 10° and 40° and a dominant peak at a 2θ angle of 26.6° which is attributed to the presence of crystalline silica in the form of quartz.

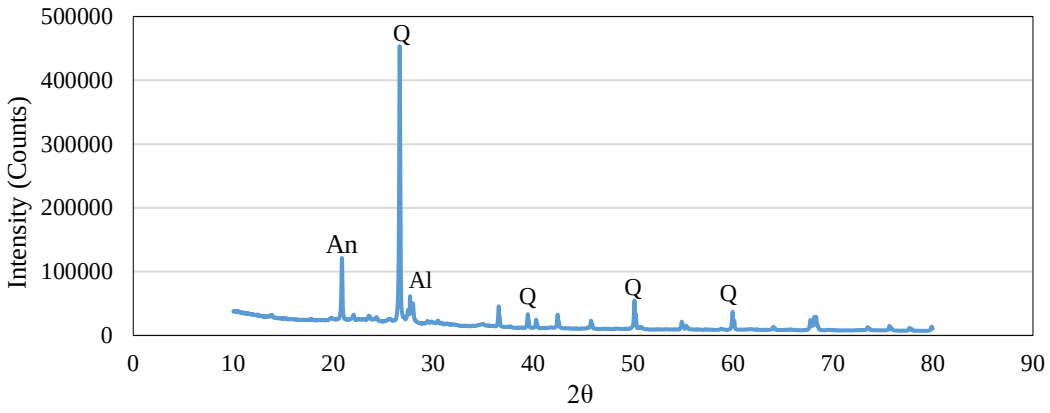

(a)

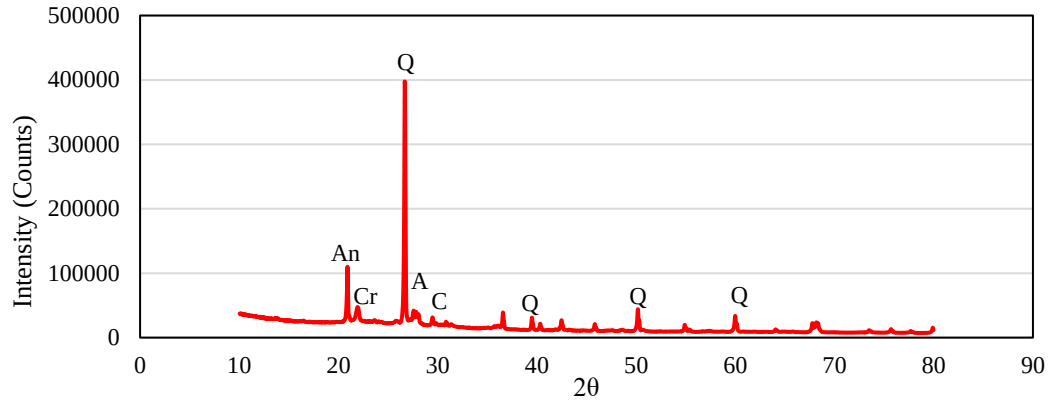

(b)

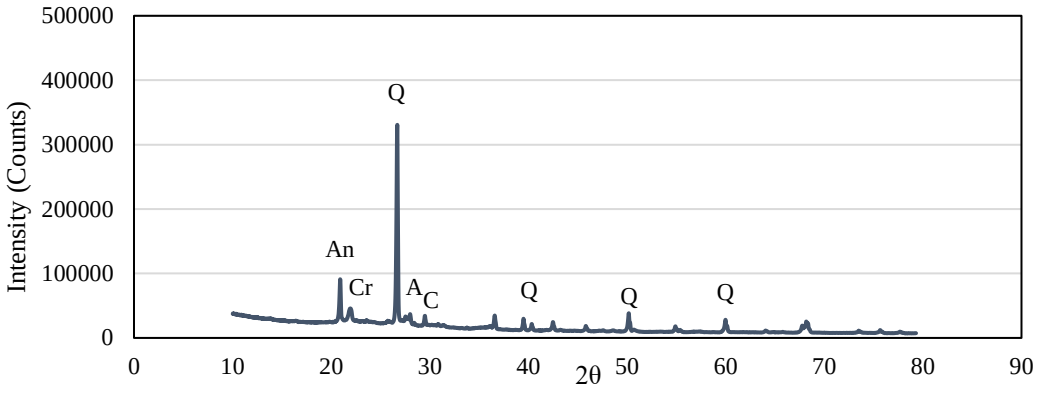

(c)

An: Anorthoclase, Cr: Cristoballite, Q: Quartz; A: Anorthite; Al: Albite, C: Calcite;

Figure 14. X-ray diffraction patterns: (a) C-450 (b) P-450 and (c) BA-U.

The phases identified in the different SCBA materials from the XRD analysis are presented in Table 7. A check symbol (✓) indicates the presence of corresponding phase. From Table 7, it should be noted that cristobalite is present in both raw and post-processed SCBA; yet, absent in controlled SCBA. As suggested by a previous study, the presence of cristobalite in bagasse ash is

related to high burning temperatures in the sugarcane factory boiler (18).Therefore, its absence in controlled SCBA its expected as this material was only burned under controlled conditions in the laboratory.

Table 7. XRD analysis for SCBA samples.

Compounds	BA-U	C-450	C-500	C-550	C-600	C-650	P-450	P-500	P-550	P-600	P-650
Quartz	✓	✓	✓	✓	✓	✓	✓	✓	✓	✓	✓
Albite, Calcian		✓	✓	✓	✓	✓		✓	✓	✓	
Anorthoclase	✓	✓	✓	✓	✓	✓	✓		✓	✓	✓
Calcite	✓						✓	✓	✓	✓	✓
Cristobalite	✓						✓	✓	✓	✓	✓
Anorthite	✓						✓				
Amorphous Component	✓	✓	✓	✓	✓	✓	✓	✓	✓	✓	✓

5.1.3. Particle Size Analysis

Laser diffraction particle size analysis was conducted for all the SCBA materials produced in this study. Tables 8 and 9 present the particle size distribution of all SCBAs before and after grinding (using a jar mill at 300 rpm for 35 minutes), respectively. From Table 8, it can be easily noticed the significant effect of post processing on reducing the particle size of raw SCBA. Raw SCBA exhibited a mean particle size of 195 µm; yet after post-processing, SCBAs exhibited mean particle sizes between 22 and 44 µm. This phenomenon is attributed to the calcination of coarse fiber impurities observed in raw SCBA during the post-processing. Furthermore, similar particle sizes to those of post-processed SCBAs were observed for controlled SCBAs which exhibited mean particle sizes between 30 to 45 µm. It is important to mention that based on the results presented in Table 8, no evident relationship between calcination temperature and particle size distribution was observed for controlled and post-processed SCBA.

Table 8. Particle size distribution for ungrinded SCBA materials.

ID	Mean (um)	Median (um)	D10 (um)	D25 (um)	D50 (um)	D75 (um)	D90 (um)
BA-U	195	266	25	80	266	534	785
C-450	31	35	4	12	35	84	159
C-500	33	37	5	13	37	89	164
C-550	30	33	5	12	33	77	140
C-600	45	49	7	18	49	119	154
C-650	34	37	6	15	37	87	161
P-450	44	27	2	9	27	61	120
P-500	28	26	4	12	26	42	52
P-550	22	29	3	8	29	36	40
P-600	32	31	5	15	31	49	58
P-650	23	23	3	10	23	36	44

Table 9 presents the particle size distribution of bagasse ash after grinding. From Table 9, a dramatic reduction in the mean particle size was identified for raw SCBA from 195 µm to 23 µm due to the effect of grinding. In the case of controlled and post-processed SCBAs, the effect of grinding was effective in eliminating coarse particles. This was noticed by the decrease in the D90 value. For controlled SCBA, D90 value ranged from 140 to 164 µm before grinding; yet, after grinding D90 value ranged between 40 and 61 µm. The same was observed for post processed SCBA where the D90 value ranged from 40 to 120 µm before grinding and between 39 and 77 µm after grinding.

Table 9. Size distribution for grinded samples.

ID	Mean (um)	Median (um)	D10 (um)	D25 (um)	D50 (um)	D75 (um)	D90 (um)
BA-U	23	27	4	11	27	52	88
C-450	27	24	2	7	22	41	61
C-500	20	14	2	4	14	32	49
C-550	17	10	1	3	10	25	44
C-600	16	11	1	4	11	24	40
C-650	20	14	2	4	14	32	49
P-450	28	24	2	8	24	45	62
P-500	34	29	3	11	29	53	72
P-550	36	32	4	13	32	57	77
P-600	33	30	4	12	30	52	68
P-650	20	19	3	8	19	32	39

In order to further illustrate the aforementioned effects of grinding, Figures 15 and 16 present graphical representations of the particle size distribution of SCBAs before and after grinding. For controlled and post-processed SCBAs only C-450 and P-450 materials are presented for clarity.

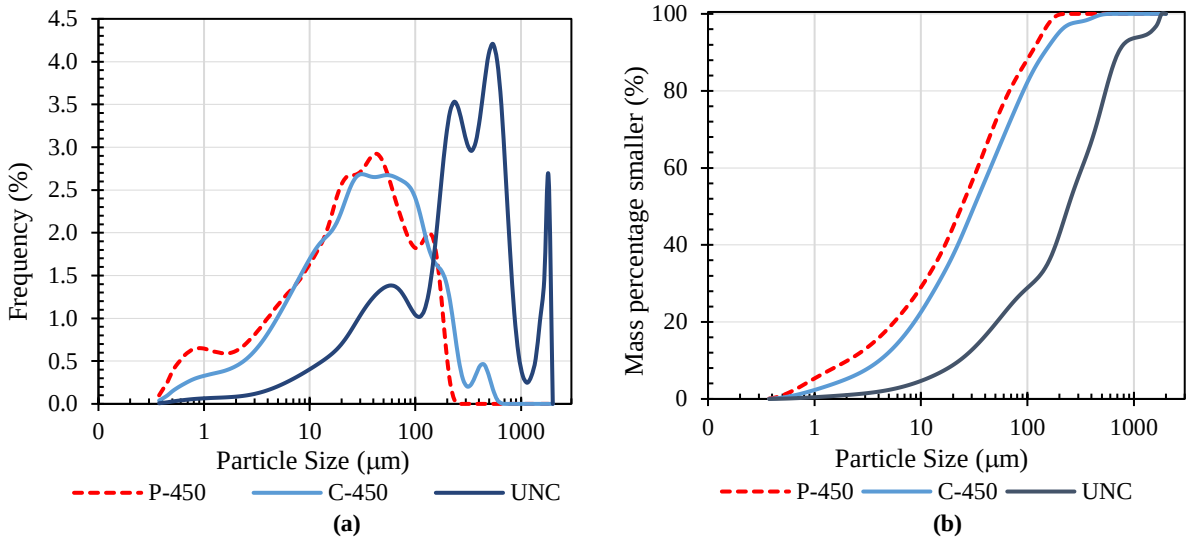

Figure 15. Ungrinded SCBAs: (a) particle size histogram and (b) cumulative particle size distribution.

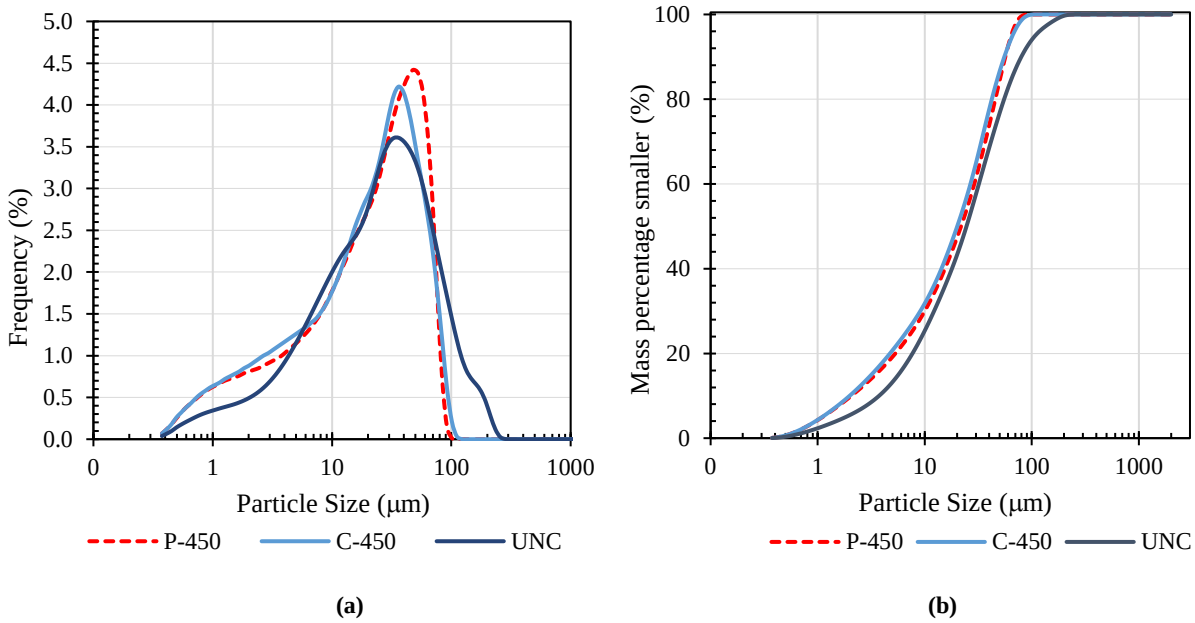

Figure 16. Grinded SCBAs: (a) particle size histogram and (b) cumulative particle size distribution.

As previously mentioned, the effect of grinding on controlled and post-processed SCBAs was mainly noticeable on the reduction of coarser particles. In Figures 15 and 16, this effect is clearly noticed. Before grinding, C-450 and P-450 exhibited particles larger than 200 and 400 µm, respectively. Yet, after grinding, particles above 100 µm were virtually eliminated in both SCBAs.

5.1.4. Moisture Content and Loss on Ignition

The moisture content (MOC) and loss on ignition (LOI) for all SCBAs are presented in Table 10. Among all SCBA materials, raw SCBA exhibited the highest MOC and LOI of 1.36 and 12.25%, respectively. The high LOI exhibited by raw SCBA was attributed to the high carbon content in the form of organic matter (i.e., unburned bagasse fibers) present in this material as demonstrated previously by SEM-EDS analysis. Previous studies also reported similar findings *(14, 18)*.

In the case of controlled SCBAs, MOC and LOI values were significantly lower than that of raw SCBA ranging from 0.54 to 1.18% and 3.48 to 1.03% for MOC and LOI, respectively. The effect of LOI reduction was expected as raw SCBA is burned under controlled conditions (small temperature gradients); thus, significantly reducing the number of unburnt particles and therefore reducing carbon content. Furthermore, it is important to notice that a clear negative relationship was observed between the burning temperature of controlled SCBA and LOI. As the calcination temperature increased, LOI decreased proportionally as shown in Figure 17. This phenomenon is attributed to an increase in the efficiency to burn organic matter as temperature increases.

For post-processed SCBAs, the MOC and LOI values were the lowest, ranging from 0.29 to 0.53% and 1.03 to 1.91% for MOC and LOI, respectively. This is explained by the double burning occurring in post-processed SCBAs (once in the sugar mill and once during the post-processing) which was expected to extract of most of the moisture and eliminate most of the organic matter in the SCBAs. Moreover, similar to what was observed in controlled SCBAs, a clear negative relationship between calcination temperature and LOI was observed (Figure 17).

Table 10. Moisture content and loss on ignition for bagasse samples.

ID	MOC (%)	LOI (%)
BA-U	1.36	12.24
C-450	1.18	3.48
C-500	0.95	2.36
C-550	0.76	1.68
C-600	0.54	1.50
C-650	0.56	1.03
P-450	0.53	1.91
P-500	0.29	1.63
P-550	0.35	1.50
P-600	0.40	1.24
P-650	0.32	1.03

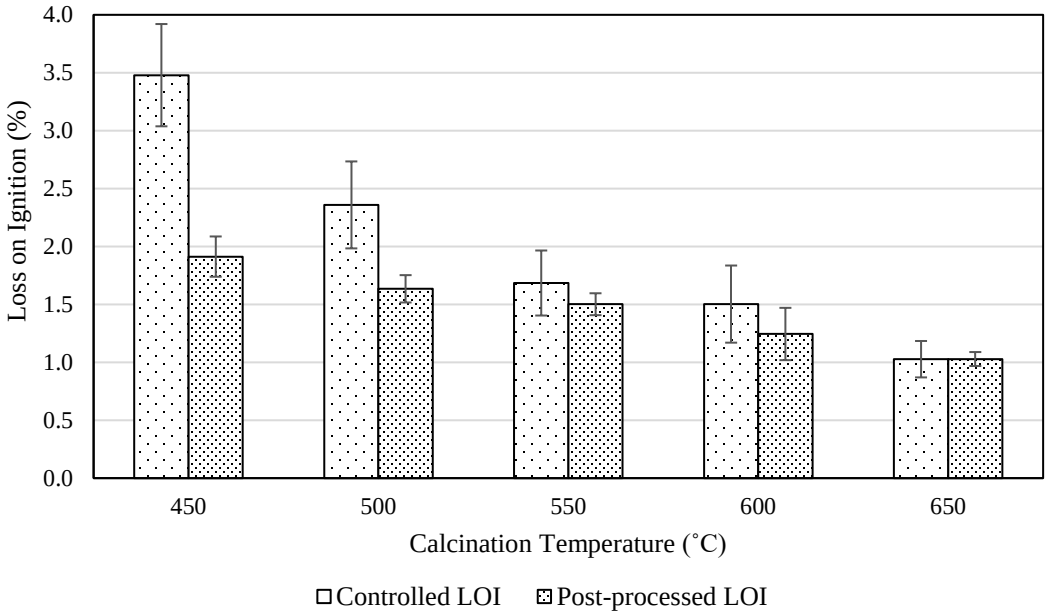

Figure 17. LOI of SCBAs.

The MOC values exhibited by all SCBAs evaluated in this study were in compliance with the maximum MOC limit of 3% established by ASTM C618. However, only controlled and post-processed SCBAs were able to meet the LOI requirements established by ASTM C618 of a maximum of 10% for Class N pozzolans and 6% for Class F and C pozzolans.

5.1.5. Strength Activity Index (SAI)

The compressive strength results of control cement mortar cubes as well as SCBA admixed cement mortar cubes (i.e., 20% cement replacement by weight per ASTM C311 guidelines) are presented in Table 11. It is important to notice that one set of mortar cubes was manufactured by replacing cement with inert silica sand (labeled as SA in Table 11). This was done in order to have a lower bound indication of pozzolanic activity. Based on the compressive strength results, SAI values were determined according to Eq.4. For better illustration, Figure 18 presents the SAI results in a graphical format.

Table 11. Strength Activity Index for Bagasse ash.

ID	Average Compressive Strength (MPa)	Standard Deviation (MPa)	Coefficient of Variation (%)	Strength Activity Index (%)
CO	42.41	3.36	7.93	-
BA-U	29.14	0.87	2.98	68.72
C-450	36.30	0.87	2.39	85.60
C-500	36.84	2.43	6.61	86.88
C-550	33.53	3.03	9.04	79.07
C-600	30.17	8.89	29.46	71.14
C-650	39.07	1.30	3.33	92.13
P-450	38.01	1.12	2.95	89.64
P-500	35.16	2.03	5.78	82.91
P-550	34.44	0.87	2.51	81.21
P-600	35.28	0.88	2.49	83.19
P-650	35.18	1.62	4.60	82.97
SA	28.33	2.12	7.48	66.81

From Figure 18, the effect of SCBA processing on the pozzolanic activity of bagasse ash can be clearly identified. For raw SCBA, the SAI value was the lowest with 68.72%. This result is in accordance with findings in previous section of this report where raw SCBA was shown to exhibit the lowest pozzolanic component, the highest MC and LOI, and coarser particle size, all of which hinder pozzolanic activity. While raw SCBA SAI was low, it is important to notice that it did not fall below the sand admixed mortar (SA) SAI value of 66.81%. Therefore, this suggested that raw SCBA presented a minor pozzolanic activity. Per ASTM C618, a minimum SAI of 75% is required for a material to be considered as a pozzolan for concrete application; thus, raw SCBA fails to adhere to this category.

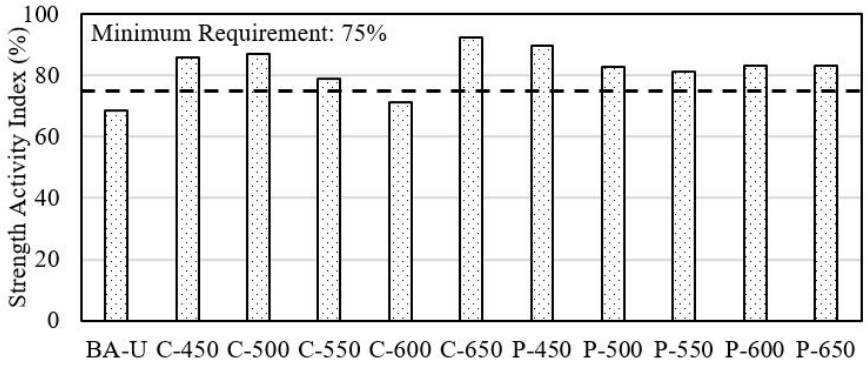

Figure 18. Strength Activity Index for different SCBAs.

In the case of controlled SCBAs, SAI values ranged from 71.14 to 92.13% with the best SAI presented at the highest calcination temperature of 650°C. This result is in accordance with findings presented previously in this report where the highest pozzolanic component and lowest LOI occurred at 650°C for controlled SCBA. Furthermore, it is important to notice that with the

exception of C-600 SCBA material, all controlled SCBAs met the minimum SAI requirement per ASTM C618.

For post-processed SCBAs, SAI values ranged from 81.21 to 89.64% with the best SAI occurring at the lowest calcination temperature of 450°C. This result was consistent with EDS findings presented previously which determined that the maximum pozzolanic component for post-processed SCBAs occurred at 450°C. Furthermore, lower calcination temperatures are likely to prevent crystallization of silica; and therefore, favor pozzolanic activity. This is particularly relevant for post-processed SCBAs since previous uncontrolled calcination in the sugar mill subjected portions of this material to high temperatures (as demonstrated by the presence of cristobalite in the XRD analysis); thus, including nonreactive crystalline silica particles in the material. In the case of post-processed SCBAs, all materials complied with the minimum SAI requirement per ASTM C618.

Among all SCBAs, C-650 exhibited the greatest SAI. However, controlled burning of SBF produces a low SCBA yield of 3 to 6%; thus, its feasibility for large-scale industrial application is challenging. On the other hand, post-processing of raw SCBA produces a significantly higher yield in the range of 85 to 90%. Therefore, preferable for large-scale production. For this reason, the best performing post-processed SCBA, P-450, was selected for further analysis (i.e., pH, water soluble sulfates, and testing in concrete). It is important to notice that a t-test was conducted to evaluate if the difference in compressive strength between C-650 and P-450 was significant. Per the t-test, no statistically significant difference was encountered ($p=0.146$).

5.1.6. pH Value

The pH evaluation was conducted on the P-450 SCBA material. Three samples were evaluated to determine the pH value. The average pH obtained was 10.01. The standard deviation and coefficient of variation were 0.035 and 0.35%, respectively. The alkalinity of the SCBA was attributed mainly to its CaO and K_2O content.

5.1.7. Water Soluble Sulfates

An experimental analysis for water-soluble sulfates was conducted on the SCBA P-450. The sulfate content obtained based on the analysis was 0.12% (by weight). This value is significantly lower than that of the maximum sulfate limit in ASTM C618 (i.e., 4% for Class N pozzolans and 5% for Class F and C pozzolans). From the EDS analysis, the total sulfate content in P-450 was 0.33%. The value from the EDS analysis reports the total sulfate content, whereas the value presented in this section presents the water-soluble sulfates.

5.2. Testing of Bagasse Ash Admixed Concrete

5.2.1. Compressive Strength

In order to evaluate the impact of the selected SCBA material (i.e., P-450) on the compressive strength of concrete, two types of concretes were produced, Class-A (i.e., 27.6 MPa target compressive strength, i.e., 4000 psi) and Class B (with 20.7 MPa target compressive strength, i.e., 3000 psi), and admixed with different contents of SCBA. The compressive strength results at 28 and 90 days of curing are presented in Figure 19. Figure 19a presents the compressive strength of the 5 different Class A mixtures (i.e., 0, 10, 20, 30 and 40% cement replacement with SCBA) while

Figure 19b presents the results for Class B mixtures (i.e., 0 and 20% cement replacement with SCBA).

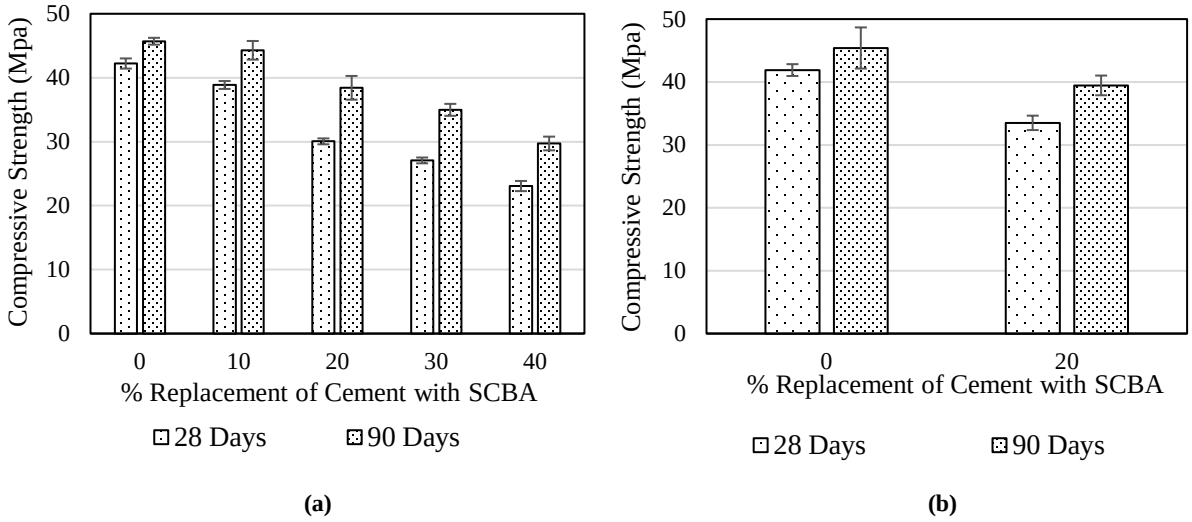

Figure 19. Compressive strength of concrete cylinders: (a) Class-A mixtures and (b) Class-B mixtures.

From Figure 19a a clear relationship was observed between compressive strength and SCBA content. As SCBA content was increased, both, the 28-day and 90-day compressive strength decreased proportionally. However, the decrease in the 90-day compressive strength was substantially smaller than that of the 28-day compressive strength as shown in Figure 20. In particular, at 10% SCBA content, the 90-day compressive strength was only 3.1% lower than that of the control mixture. Furthermore, based on an ANOVA and Tukey Pairwise Comparison of Class-A concrete mixtures, the difference between the 90-day compressive strength of the control mixture and the 10% SCBA mixture was not statistically significant. It is important to mention that this was the only non-significant difference encountered in the analysis.

One important characteristic of the SCBA admixed concrete mixtures was the enhanced relative compressive strength gain from 28 to 90 days (Figure 21). As shown in Figure 21, a dramatic enhancement in the relative strength gain was observed as the SCBA content increased up to 20%. However, after reaching the 20% SCBA content, the relative strength gain enhancement seemed to stabilize. An ANOVA and Tukey Pairwise Comparison was conducted to evaluate if the differences in relative strength gain between control and SCBA admixed concrete mixtures were significant. Per the analysis, a statistically significant difference was encountered for the relative strength gain between the control mix and SCBA admixed concrete mixtures utilizing SCBA at 20, 30, and 40% cement replacement.

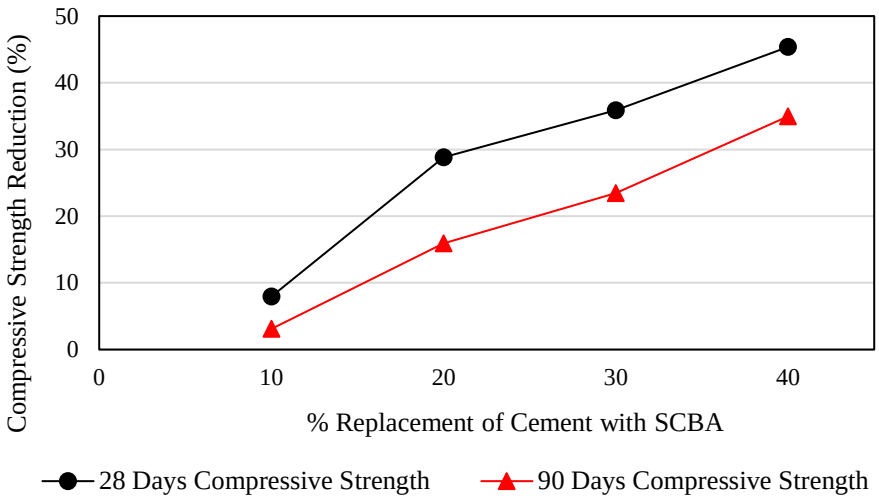

Figure 20. Reduction in compressive strength with different levels of cement replacement with SCBA for Class-A concrete mixtures.

As shown in Figure 19b, a clear decrease in compressive strength was observed in Class-B mixtures at, both, 28 and 90 days due to the 20% cement replacement with SCBA. However, the compressive strength decreases at 90 days (i.e., 13.1%) was lower than the decrease at 28 days (i.e., 20.0%). Furthermore, similarly to what was observed for Class-A concrete mixtures, the relative strength gain from 28 to 90 days was significantly enhanced by the addition of SCBA. For the control mixture the relative gain was 8.40%; yet, for the concrete mixture with 20% cement replacement with SCBA the relative gain was of 17.8%. Moreover, a t-test was conducted to evaluate if the differences in compressive strength between control and SCBA admixed concrete was significant for Class-B mixtures. Per the t-test, a statistically significant difference was encountered (p=0.0006) for the compressive strength at 28 days; however, at 90 days the difference between control and the mixture with 20% cement replacement with SCBA was not statistically significant (p= 0.0668).

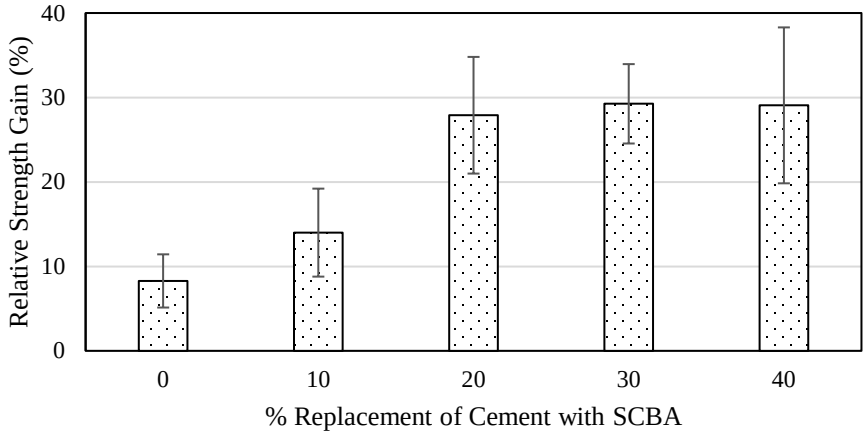

Figure 21. Relative compressive strength gains from 28 to 90 days at different levels of cement replacement with SCBA for Class-A concrete mixtures.

The compressive strength reductions observed in Class-A and Class-B concrete mixtures containing SCBA were expected as the SAI of the SCBA material utilized as cement replacement was lower than 100%. Moreover, the enhancement in long term compressive strength performance (i.e., 90 days) of SCBA admixed concrete mixtures was attributed to the pozzolanic activity of SCBA. As the curing process progresses, the amorphous silica in SCBA reacts with calcium hydroxide (CH) from cement hydration to form calcium-silicate-hydrate (CSH). This pozzolanic effect enhances the pore structure of concrete, which ultimately contributes towards the higher long-term compressive strength *(5, 40)*. It is important to mention that the increase in compressive strength may be also partially attributed to the filler effect of SCBA. Due to its fine particle size, SCBA can act as a mineral filler in concrete mixtures, improving particle packing; and thus, leading to the enhancement of concrete compressive strength.

The stabilization in the enhancement of relative strength gain observed in Class-A mixtures after 20% replacement of cement with SCBA, was attributed to a decrease in the availability of CH from cement hydration reaction (due to cement content decrease) and an increase in the CH demand by the increasing pozzolanic component. Hence, leading to the unavailability of sufficient CH for the pozzolanic reaction at later ages *(41)*.

5.2.2. Surface Resistivity

In order to gain insight on the potential durability enhancements provided by the addition of pozzolanic components such as SCBA in concrete, surface resistivity test was conducted. Figure 22 presents the surface resistivity values obtained for the different concrete mixtures evaluated in this study. From Figure 22a, an interesting trend was observed in Class-A concrete mixtures, as SCBA content increased, the 90-day surface resistivity value increased proportionally. Moreover, for the control mixture, the 90-day surface resistivity value (i.e., 13.1 KOhm-cm) fell in the category of moderate chloride ion penetrability per DOTD TR233. However, at 40% cement replacement with SCBA the surface resistivity value (i.e., 23.5 KOhm-cm) fell in the category of low chloride penetrability. These findings highlight the significance of pozzolanic materials such as SCBA in increasing the durability of concrete. In the case of Class-B concrete mixtures, an important increase in surface resistivity was also observed at 90 days due to the addition of SCBA as shown in Figure 22b. At 90 days of curing, the control mixture exhibited a surface resistivity value of 14.5 KOhm-cm; yet, the mixture containing a 20% cement replacement with SCBA exhibited a 19.9 KOhm-cm surface resistivity value (i.e. a 37.2% increase compared to control). The enhancements in durability potential of concrete with SCBA are explained by the improved pore structure provided by the pozzolanic reaction of SCBA.

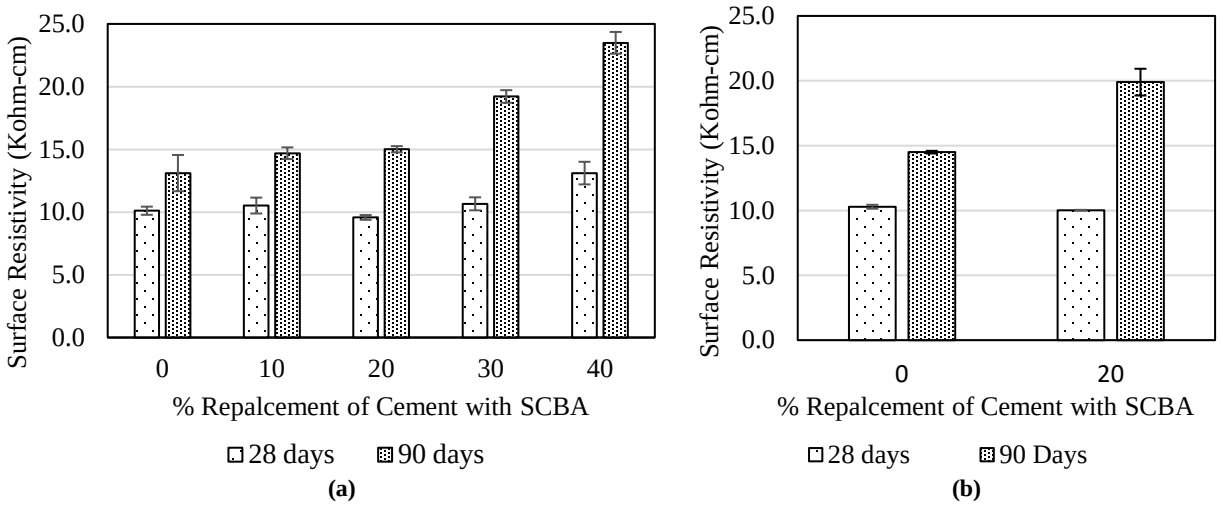

Figure 22. Surface resistivity for concrete cylinders: (a) Class-A mixtures and (b) Class-B mixtures.

5.2.3. Slump and Unit Weight

The workability and unit weight of fresh concrete were evaluated in this study by the slump and unit weight tests per ASTM C143 *(42)* and ASTM C138 *(43)*, respectively. Slump and unit weight results for all concrete mixtures in this study are presented in Figures 23 and 24.

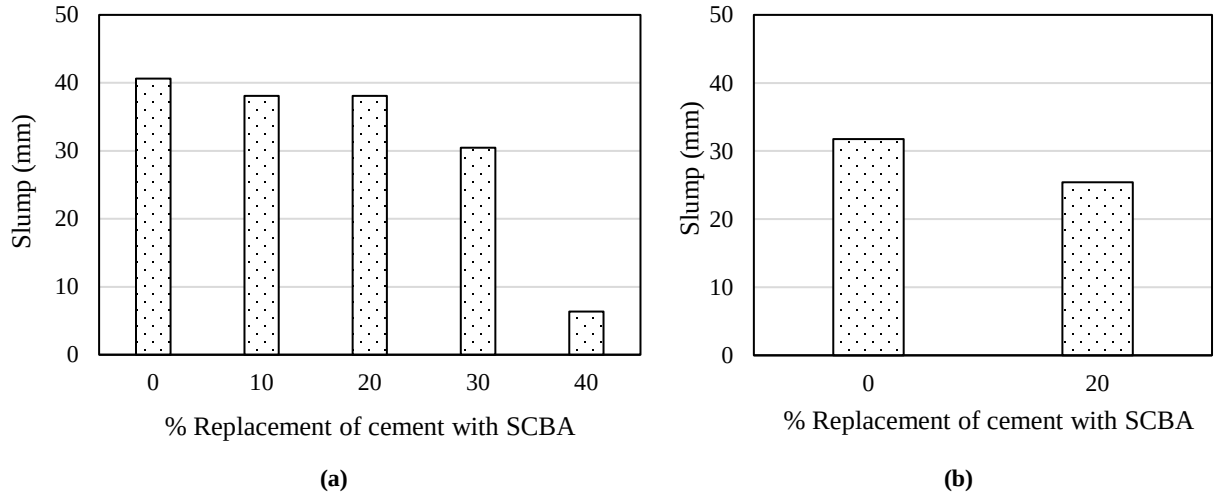

Figure 23. Slump at different levels of cement replacement with SCBA: (a) Class-A and (b) Class-B.

Figure 23 presents the effect of SCBA on the workability of the concrete mixtures at a constant water-to-binder ratio of 0.48. From Figure 23, it was clearly noticed that the addition of SCBA negatively affected workability. As SCBA content increased, workability decreased proportionally. This effect was observed for, both, Class-A and Class-B concrete mixtures. The evident decrease in workability suggested that SCBA mixtures require more water than the control mixture to achieve a similar workability. The observed increase in the water demand can be attributed due to the porous nature of the SCBA particles (porous particles observed in SEM) and their greater specific surface area in comparison to the cement *(41)*. Furthermore, the irregular shape and rough surface of SCBA particles may reduce the packing density and increased the

interstitial voids in fresh concrete; thus, increasing the amount of water required to lubricate the surface of the particles *(14)*.

From Figure 24, it can be observed that the addition of SCBA produced a clear decrease in the unit weight of concrete for, both, Class-A and Class-B mixtures. This reduction in unit weight was expected due to the lower density of SCBA as compared to cement.

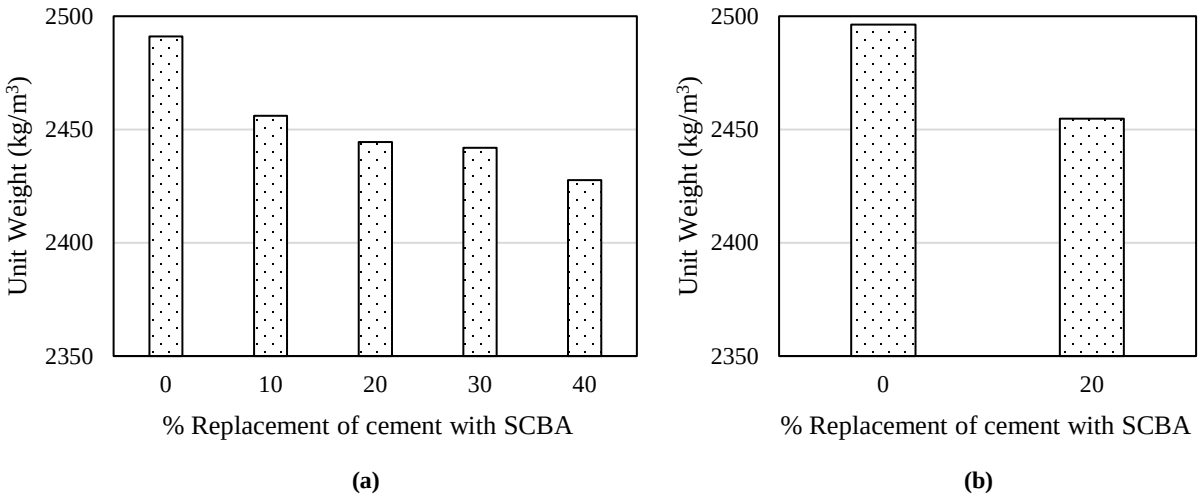

Figure 24. Unit Weight at different levels of cement replacement with SCBA: (a) Class-A and (b) Class-B.

5.2.4. Drying Shrinkage

Figure 25 present the drying shrinkage results of Class-A and Class-B concrete mixtures after 7, 14, and 28 days of curing in lime saturated water. From Figure 25, it can be observed that the drying shrinkage for Class-A and Class-B controlled mixtures, was lower than that of the mixtures containing SCBA at all ages of curing (with the exception of Class-A mixture at 20% cement replacement with SCBA after 14 days of curing). One of the primary sources of drying shrinkage is due to the loss of capillary water held in cement pastes *(44)*. The cement replacement with SCBA reduces the cement content; thus, lowering the amount of hydration products. In turn, this leads to the availability of more water in capillary pores of the hydrated cement pastes *(44)*. The availability of pore water, in combination with the presence of amorphous silica in significant quantities can trigger a pozzolanic reaction and consumption of pore water. Due to this phenomena, concrete containing SCBA likely exhibited an increase in drying shrinkage *(45)*. As shown in Figure 25, shrinkage in all concrete mixtures increased with curing time as expected (with the exception of Class-A concrete at 20% SCBA content, where the 14 days shrinkage value was lower than the 7 days value). However, SCBA admixed concretes (excepting Class-A mixture at 20% cement replacement with SCBA after 14 days of curing) exhibited a particularly enhanced drying shrinkage at early stages of the curing process (i.e., 7 and 14 days). This phenomenon could be partially attributed to the highly porous nature of SCBA which could potentially absorb water and increase drying shrinkage at early ages. It is important to mention that after 28 days of curing increases in drying shrinkage due to SCBA addition were small.

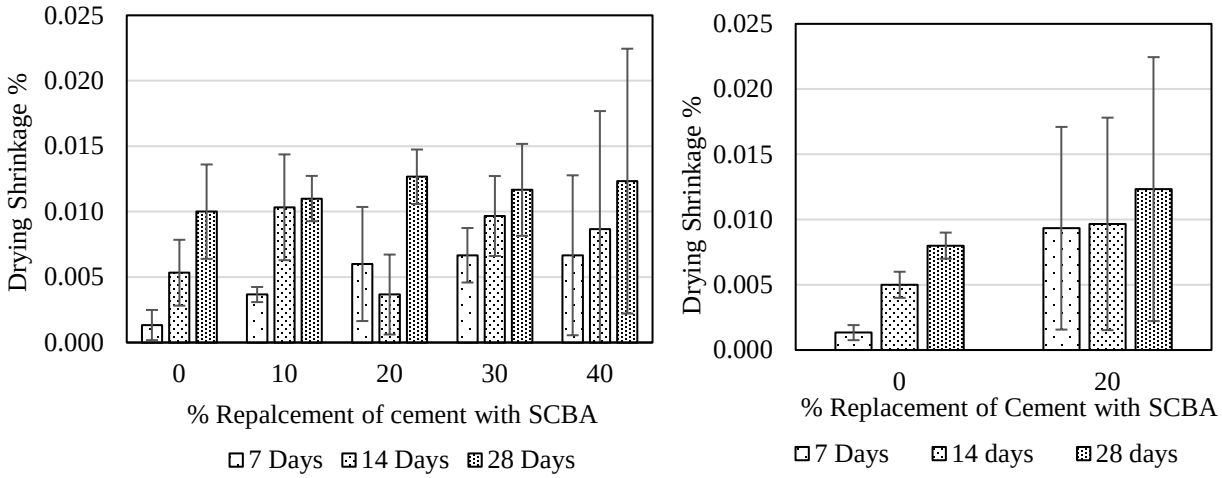

(a) **(b)**

Figure 25. Drying shrinkage at different levels of cement replacement with SCBA: (a) Class-A and (b) Class-B.

In the case of Class-A concrete, the shrinkage values obtained at 28 days for all concrete mixtures admixed with SCBA were relatively low and well within the upper limit stablished by the Louisiana Standard Specification for Roads and Bridges of 0.07% (at 28 days) for structural concrete patching materials *(46*). Furthermore, no evident trend was observed between shrinkage and increasing contents of SCBA. In the case of the SCBA admixed Class-B concrete mixture, the shrinkage limit stablished by the Louisiana Standard Specification for Roads and Bridges for structural concrete patching materials was also met. It is important to note that there was a high variability in the drying shrinkage results. Hence, a robust conclusion cannot be drawn from these results. For future research, extensive drying shrinkage experimentation is required to validate the results presented in this report.

5.2.5. Water Absorption

The water absorption of each concrete mixture was evaluated after 28 days of curing per ASTM C642 guidelines. Figure 26 presents the water absorption results for all the concrete mixtures evaluated in this study. As shown in Figure 26, water absorption increased with the addition of SCBA. This was true for Class-A and Class-B concrete mixtures.

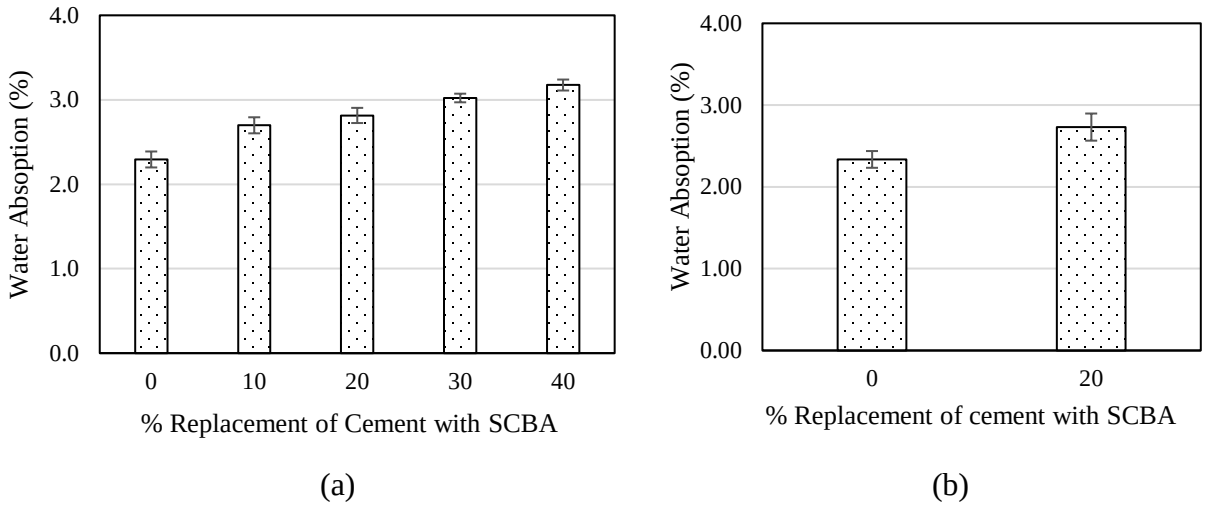

Figure 26. Water Absorption at different levels of cement replacement with SCBA: (a) Class-A and (b) Class-B.

The increase in water absorption with SCBA content is attributed to the porosity of SCBA *(40)*. Porous materials such as SCBA tend to absorb more water; thus, contributing to the overall water absorption of concrete. In addition, water absorption of concrete was measured at a relatively young age (i.e., 28 days); thus, the pozzolanic reaction of SCBA was limited at the time of testing. It is expected that at later ages of curing, results will differ significantly to those presented in Figure 26 due to the enhancement of the porous structure of concrete admixed with SCBA (due to the pozzolanic reaction). A clear example of this phenomena was previously observed in the surface resistivity section of this report, were surface resistivity values of concrete mixtures with SCBA at 28 days of curing were in some cases lower than those of control. However, at 90 days of curing surface resistivity values of concrete mixtures with SCBA increased significantly and outperformed control in all cases.

5.3. Cost Analysis of SCBA Admixed Concrete

In a competitive industry like the transportation industry, it is important to quantify the economic performance of SCBA concrete versus regular concrete. Therefore, a comparative cost analysis was performed on a typical 225-mm (9-in) Jointed Plain Concrete Pavement (JPCP) constructed using a typical concrete mix used in LA versus a SCBA concrete. For the purpose of the cost analysis, it is assumed that the SCBA concrete will have similar performance to regular concrete. Therefore, operation and maintenance costs for both cases (regular concrete and SCBA) are considered the same and not considered as part of this analysis. The main difference in cost is expected to result from replacing the cement with bagasse ash.

A case study of a JPCP pavement, constructed in 2015 in East Baton Rouge Parish was considered in the cost analysis. The project was constructed with an annual average daily traffic (AADT) of 21,864 and the pavement section consisted of three layers: a class D geotextile fabric, a 200-mm Class II base course (crushed stone or recycled PCCP), and a 225-mm thick top layer of Portland Cement Concrete (PCC). The compressive strength of 225-mm thick PCC layer was 32.61 MPa. In cost analysis, all other design parameters, except mix design, of regular and SCBA concrete is assumed to be same. Construction cost data for the JPCP constructed with regular type I cement were obtained from Louisiana Department of Transportation and Development (LaDOTD) bidding cost history database and are summarized in Table 12. Material price for concrete, presented in Table 12, were calculated based on average price of concrete mix ingredients in Louisiana. As shown in Table 12, the average construction cost of a regular 9-in JPCP pavement is $102.13 per m^2 (85.39 per yd^2), i.e. $597.7K for 1 lane-mile of regular concrete.

Table 12. Average construction and material cost for regular concrete pavements *(47)*.

Description	Material Price ($ per m^2)	Average Construction price ($ per m^2)
8” Thick JPCP	31.48	85.00
9” Thick JPCP	35.41	102.13
10” Thick JPCP	39.35	133.95

Based on the results of this study, the cost analysis assumes a 10% cement replacement with SCBA in concrete. All other mix ingredients in SCBA concrete are considered the same as those used for typical concrete. Since bagasse ash is considered a waste product, the cost of the bagasse ash was calculated by quantifying three parameters as shown in Table 13:

1. Transportation cost from the Alma sugar plantation located in Baton Rouge LA to concrete plant location, a 39.5 km distance.
2. Cost of grinding the bagasse ash by assuming that electricity consumption will be similar to that of the cement grinding procedure.
3. Cost of burning the raw SCBA using an industrial kiln (as in cement) to produce post-processed SCBA using Equation 7,

$$T = P\ X\ U \qquad [7]$$

where,
T= Total cost of burning to produce 1 metric ton of post-processed SCBA (P-450) in $
P = Total energy consumed for burning (kWh)

U = Average industrial electricity rate for Louisiana ($ per kWh)

Table 13. Material production cost for post-processed SCBA *(48–51)*.

Description	Value	Units
Cost for Material Transportation	0.039	Cost per metric ton per km for standard truck
Alma Plantation to concrete plants (Average Distance from Alma Plantation to nearby Plants)	39.5	Km
Total Cost for transportation of 1 ton of bagasse	1.56	$ per ton
Total Power Consumption	1000	kWh
Average Retail Price for Louisiana	5.39	(cents/kWh)
Cost of burning	53.90	$
Electrical Consumption for Grinding	77	Kilowatt hours per metric ton
Cost for Grinding (Electrical Only)	4.15	$ per metric ton
Total cost per ton	59.61	$ per metric ton

As shown in Table 13, the material production cost for post-processed (P-450) is $59.61 per metric ton (an 85% SCBA yield during the burning process was assumed). Assuming a cement cost of $172.18 per metric ton, the cost of SCBA is 65.38% more effective.

The cost of SCBA concrete with 10% SCBA cement replacement is shown in Table 14. Based on the cost analysis, the price of concrete with SCBA is $101.37 per m^2 or $593.2K per lane-mile. Assuming a concrete cost of $597.7K per lane-mile, the use of SCBA as a 10% replacement of cement in concrete will result in a cost saving of approximately $4,462.2 or 0.75% per lane mile of installed concrete.

Table 14. Cost Analysis for SCBA concrete mix.

Description	Value	Unit
Price of regular concrete construction	102.13	per m^2
Price of regular concrete construction	446.78	per m^3
Cement content in concrete	296.30	kg/m^3
Price of cement	172.18	$ per metric ton
Price of cement in concrete	51.02	$/m^3$
Price of SCBA	59.61	$ per metric ton
SCBA content in concrete	29.63	kg/m^3
Price of bagasse ash in SCBA concrete	1.77	$/m^3$
Cement content in SCBA concrete	266.67	kg/m^3
Price of cement in SCBA concrete	45.91	$/m^3$
Price of 10% SCBA concrete	443.44	per m^3
Price of 10% SCBA concrete	101.37	per m^2
Total construction cost of 1 lane mile of SCBA concrete pavement	593,244	$ per lane-mile
Total construction cost of 1 lane mile of regular concrete pavement	597,706	$ per lane-mile
Expected Cost Saving per lane-mile	**4,467**	$ per lane-mile

6. CONCLUSIONS

Several SCBA materials were successfully produced utilizing different processing methodologies and thoroughly characterized. Furthermore, SCBA material P-450 was evaluated in concrete mixtures. Based on the experimental results, the following conclusions can be drawn:

- Raw SCBA presented unsatisfactory pozzolanic activity (SAI of 68.72%) failing to meet ASTM C618 minimum SAI requirement to be classified as a SCM. In addition, raw SCBA also failed to meet ASTM C618 requirements for pozzolanic component and LOI. The low pozzolanic activity of raw SCBA and its failure to meet pozzolanic component and LOI requirements was mainly attributed to its high carbon content.

- The post-processing of raw SCBA by further burning, increased the pozzolanic activity of SCBA significantly and allowed all post-processed SCBAs to exceed the minimum SAI requirement per ASTM C618. Furthermore, all post-processed SCBAs met ASTM C618 requirements for pozzolanic component, LOI and moisture content. The enhancement in pozzolanic activity was mainly attributed to the removal of carbon. Moreover, the post-processing calcination temperature producing the best pozzolanic activity (SAI of 89.64%) was 450°C (P-450).

- With the exception of C-600, all controlled SCBA materials exhibited satisfactory pozzolanic activity meeting ASTM C618 minimum SAI requirements. Furthermore, ASTM C618 requirements for pozzolanic component, LOI, and moisture content, were met by all controlled SCBAs. The best pozzolanic activity for controlled SCBAs (SAI of 92.13 %) was obtained at a calcination temperature of 650°C (C-650 exhibited).

- While C-650 SCBA presented a slightly better pozzolanic activity to that of P-450 SCBA, the difference in pozzolanic activity between these two materials was not statistically significant. Furthermore, P-450 SCBA was selected for further study in concrete mixtures due to its higher production yield which makes this material more attractive for large-scale application.

- For Class-A concrete mixtures, increasing contents of SCBA produced a decrease in, both, the 28-day and 90-day compressive strengths. However, the 90-day surface resistivity and the relative strength gain from 28 to 90 days was significantly enhanced by the increments in SCBA content. Furthermore, it was determined that utilizing a 10% substitution of cement with post-processed SCBA produced a similar compressive strength to that of the control mixture after 90 days of curing (no statistically significant difference was encountered). The enhancements in long-term strength gain (i.e., from 28 to 90 days) and long-term surface resistivity (i.e., 90 days) were attributed to pore structure refinement due to the pozzolanic activity of SCBA.

- For Class-B concrete mixtures, 20% cement replacement with P-450 SCBA produced a decrease in, both, the 28-day and 90-day compressive strengths. However, similarly to what was observed for Class A mixtures, the 90-day surface resistivity and the relative strength gain from 28 to 90 days was significantly enhanced. Furthermore, the difference

in compressive strength at 90 days between control concrete mixture and the SCBA admixed concrete mixture was not statistically significant. The enhancements in long-term strength gain and long-term surface resistivity were attributed to the pozzolanic activity of SCBA.

- The workability of fresh concrete admixed with SCBA was reduced for, both, Class-A and Class-B concrete mixtures. This was attributed to the porous nature and irregular shape of SCBA particles. Furthermore, the unit weight of fresh concrete with SCBA was reduced due to the lower density of SCBA compared to cement.

- The partial replacement of cement with SCBA produced an increase in drying shrinkage. The increase was minor after 28 days of curing. Yet, particularly noticeable at early stages of curing (i.e., 7 and 14 days). While drying shrinkage was slightly increased with the addition of SCBA, drying shrinkage values of all SCBA admixed concrete mixtures (Class-A and Class-B) were well within the limit for structural concrete patching materials per the Louisiana Standard Specification for Roads and Bridges.

- The water absorption of concrete mixtures with SCBA (Class-A and Class-B) was greater to that of regular concrete at 28-days. The increase in water absorption with SCBA content was attributed to the porosity of SCBA. However, it is expected that at later curing ages, results will differ significantly due to the enhancement of the porous structure of concrete admixed with SCBA (due to the pozzolanic reaction).

- Based on a cost analysis, it was concluded that concrete mixtures containing SCBA could be economically feasible for its implementation in pavement infrastructure. Per the analysis, the utilization of concrete with a 10% cement replacement with SCBA produced a reduction of the per lane-mile cost of 0.75%.

- Based on the results of this study, an evaluation of large-scale SCBA production is recommended to verify the feasibility of SCBA production and the consistency of its properties at an industrial scale.

REFERENCES

1. American Sugar Cane League. *Louisiana Sugarcane Industry Production Data 1975 to 2016.* American Sugar Cane League, Thibodaux, LA. 2017.

2. U.S. Department of Energy. *U.S. Billion-Ton Update: Biomass Supply for a Bioenergy and Bioproducts Industry.* RD Perlack and BJ Stokes (Leads) Oak Ridge National Laboratory, Oak Ridge, TN, 2011. Available from: http://bioenergykdf.net Accessed on Jan. 18, 2019

3. Clarke S, Preto F. *Biomass Burn Characteristics.* Ministry of Agriculture, Food, and Rural Affairs, Ontario, 2015. http://www.range-road.ca/Documents/Biomass Burn Characteristics.pdf Accessed on Jan. 20, 2018

4. Modani P.O., Vyawahare M.R. Utilization of bagasse ash as a partial replacement of fine aggregate in concrete. *Procedia Engineering,* 2013. 51: 25-29

5. Ramezanianpour A.A. *Cement Replacement Materials: Properties, Durability, Sustainability.* Springer, New York, 2014.

6. Boateng A.A., Skeete D.A. Incineration of Rice Hull for Use as a Cementitious Material: The Guyana Experience. *Cement and Concrete Research*, 1990. 20(5):795–802.

7. Zhang, M.H., Malhotra V.M. High-Performance Concrete Incorporating Rice Husk Ash as a Supplementary Cementing Material. *ACI Materials Journal*, 1997. 93(1):629–36.

8. Portland Cement Association (PCA). *Louisiana Cement Industry 2015*. Skokie, Illinois, 2016.

9. ASTM C618. *Standard Specification for Coal Fly Ash and Raw or Calcined Natural Pozzolan for Use in Concrete*. ASTM International, West Conshohocken, PA. 2010. 3–6.

10. American Road & Transportation Builders Association, *Production and Use of Coal Combustion Products in the U.S. - Market Forecast Through 2033.* American Coal Ash Association, 2015.

11. American Coal Ash Association. Fly Ash Facts for Highway Engineers. *Journal of Chemical Information and Modeling,* 2013. 53(9): 1689–99.

12. Ganesan K., Rajagopal K., Thangavel K. Evaluation of bagasse ash as supplementary cementitious material. *Cement and Concrete Composites,* 2007. 29(6): 515–24.

13. Montakarntiwong K., Chusilp N., Tangchirapat W., Jaturapitakkul C. Strength and heat evolution of concretes containing bagasse ash from thermal power plants in sugar industry. *Materials and Design,* 2013. 49: 414–20.

14. Sua-Iam G., Makul N. Use of increasing amounts of bagasse ash waste to produce self-compacting concrete by adding limestone powder waste. *Journal of Cleaner Production,* 2013. 57: 308–19.

15. Amin N. Use of Bagasse Ash in Concrete and Its Impact on the Strength and Chloride Resistivity. *Journal of Materials in Civil Engineering,* 2010. 23(5): 717–20.

16. Srinivasan R., Sathiya K. Experimental Study on Bagasse Ash in Concrete. *International*

Journal for Service Learning in Engineering, Humanitarian Engineering and Social Entrepreneurship. 2018;5(2):60–6.

17. Cordeiro G.C., Toledo Filho R.D., Fairbairn E.M.R. Effect of calcination temperature on the pozzolanic activity of sugar cane bagasse ash. *Construction and Building Materials*, 2009. 23(10) :3301–3

18. Cordeiro G.C., Toledo Filho R.D., Tavares L.M., Fairbairn E. Ultrafine grinding of sugar cane bagasse ash for application as pozzolanic admixture in concrete. *Cement and Concrete Research*, 2009. 39(2): 110–5

19. Hernandez J.F., Middendorf B., Gehrke M., Bedelmann H. Use of Wastes of the Sugar Industry as Pozzolana in Lime-Pozzolana Binders: Study of the Reaction. *Cement and Concrete Research*, 1998. 99(11) :391.

20. Payá J., Monzó J., Borrachero M. V., Díaz-Pinzón L., Ordónez L.M. Sugar-cane bagasse ash (SCBA): Studies on its properties for reusing in concrete production. *Journal of Chemical Technology and Biotechnology*, 2002. 77(3) :321–5.

21. Bahurudeen A., Santhanam M. Influence of different processing methods on the pozzolanic performance of sugarcane bagasse ash. *Cement and Concrete Composites*, 2015. 56: 32–45

22. Govindarajan D, Jayalakshmi G. XRD , FTIR and Microstructure Studies of Calcined Sugarcane Bagasse Ash. *Advances in Applied Science*, 2011. 2(3): 544–9.

23. Govindarajan D., Jayalakshmi G. XRD , FTIR and SEM studies on calcined sugarcane bagasse ash blended cement. *Archives of Physics Research*, 2011. 2(4): 38–44.

24. ASTM C150/ C150M. *Standard Specification for Portland Cement.* ASTM International, West Conshohocken, PA, 2017.

25. ASTM C778. *Standard Specification for Standar Sand*. ASTM International, West Conshohocken, PA. 2017;14:1–3.

26. Beckman Coulter Inc. *Beckman Coulter Ls Series*. Manual, 2011.

27. ASTM C311/C311M. *Standard Test Methods for Sampling and Testing Fly Ash or Natural Pozzolans for Use in Portland-Cement Concrete*. ASTM International, West Conshohocken, PA. 2005;04.02:204–12.

28. ASTM D5239. *Standard Practice for Characterizing Fly Ash for Use in Soil Stabilization. ASTM International*, ASTM International, West Conshohocken, PA. 2004.

29. ASTM D1293. *Standard Test Methods for pH of Water*. ASTM International, West Conshohocken, PA. 2018.

30. Horkoss S., Escadeillas G., Lteif R. The effect of the source of cement SO 3 on the expansion of mortars. *Case Studies in Construction Material*, 2016. 4(1): 62–72.

31. ASTM C114. *Standard Test Methods for Chemical Analysis of Hydraulic Cement*. ASTM International, West Conshohocken, PA, 2018.

32. ASTM C1437. *Test method for slump of hydraulic cement concrete*. ASTM International,

West Conshohocken, PA, 2005.

33. ASTM 192/192M A. *Standard Practice for Making and Curing Concrete Test Specimens in the Laboratory*. ASTM International, West Conshohocken, PA, 2018.

34. ASTM C109/109M. *Standard Test Method for Compressive Strength of Hydraulic Cement Mortars (Using 2-in. or [50-mm] Cube Specimens)*. ASTM International West Conshohocken, PA, 2016.

35. Louisiana Department of Transportation and Development. *Part IX- Portland Cement Concrete*. Louisiana Department of Transportation and Development, Baton Rouge, LA, 2006.

36. ASTM C157/157M. *Standard Test Method for Length Change of Hardened Hydraulic-Cement Mortar and Concrete*. ASTM International, West Conshohocken, PA, 2016.

37. ASTM C39/C39M. *Standard Test Method for Compressive Strength of Cylindrical Concrete Specimens*. ASTM International, West Conshohocken, PA, 2016.

38. Louisiana Department of Transportation and Development TR233. *Surface Resistivity Indication of Concrete's Ability to Resist Chloride Ion Penetration.* Louisiana Department of Transportation and Development, Baton Rouge, LA, 2018.

39. ASTM C642. *Standard Test Method for Density , Absorption , and Voids in Hardened Concrete*. ASTM International West Conshohocken, PA, 2013.

40. Isaia G.C., Gastaldini A.L.G., Moraes R. Physical and pozzolanic action of mineral additions on the mechanical strength of high-performance concrete. *Cement and Concrete Composites*, 2003. 25(1): 69–76.

41. Chi M.C. Effects of sugar cane bagasse ash as a cement replacement on properties of mortars. *Science and Engineering of Composite Materials*, 2012. 19(3): 279–85.

42. ASTM C143/ 143M. *Standard Test Method for Slump of Hydraulic-Cement Concrete*. ASTM International, West Conshohocken, PA, 2015.

43. ASTM C138/C138M. *Standard Test Method for Density (Unit Weight), Yield , and Air Content (Gravimetric).* ASTM International, West Conshohocken, PA, 2019.

44. Chatveera B., Lertwattanaruk P. Durability of conventional concretes containing black rice husk ash. *Journal of Environmental Managemen*t, 2011. 92(1): 59–66.

45. Cheah C.B., Ramli M. Mechanical strength , durability and drying shrinkage of structural mortar containing HCWA as partial replacement of cement. *Construction and Building Materials* , 2012. 30: 320–9.

46. Louisiana Department of Transportation and Development. *Louisiana Standard Specification for Roads and Bridges*. State of Louisiana Department of Transportation and Development, Baton Rouge, Louisiana, 2016.

47. Louisiana Department of Transportation and Development. *Cost Estimating Tools*. State of Louisiana Department of Transportation and Development, Baton Rouge, Louisiana, 2018.

48. Oss V. Cement. *US Geological Survey,* 2013. June:1–34.

49. Edision Electric Institute. *Typical Bills and Average Rates Report-Summer 2018*. Pennsylvania, 2018. https://www.rockymountainpower.net/about/rar/ipc.html Accessed Jan 12, 2019

50. Bienkowski B.N., Walton C.M. *The Economic Efficiency of Allowing Longer Combination Vehicles in Texas 7*. No. SWUTC/11/476660-00077-1. Southwest Region University Transportation Center (US), 2011.

51. Natural Resources. *Energy Consumption Benchmark Guide: Cement Clinker Production.* Office of Energy Efficiency Natural Resources, Canada, 2016

APPENDIX A: SAI STATISTICAL ANALYSIS

Table A1. t-test for C-650 and P-450 mortars compressive strength at 28 days.

Description	P-450	C-450
Mean	39.0668	38.0131
Variance	1.6911	1.2588
Observations	6	6
Hypothesized Mean Difference	0.05	
df	10	
t Stat	-1.5740	
P(T<=t) one-tail	0.0732	
t Critical one-tail	1.8124	
P(T<=t) two-tail	0.1465	
t Critical two-tail	2.2281	

APPENDIX B: STATISTICAL ANALYSIS OF CONCRETE CYLINDERS COMPRESSIVE STRENGTH (CLASS-A)

Table B1. Class A concrete cylinders 28 days compressive strength one-way ANOVA results.

Source	DF	Sum of Squares	Mean Square	F Value	Pr > F
Model	4	777.9003	194.4750	471.10	<.0001
Error	10	4.1280	0.4128		
Corrected Total	14	782.0283			

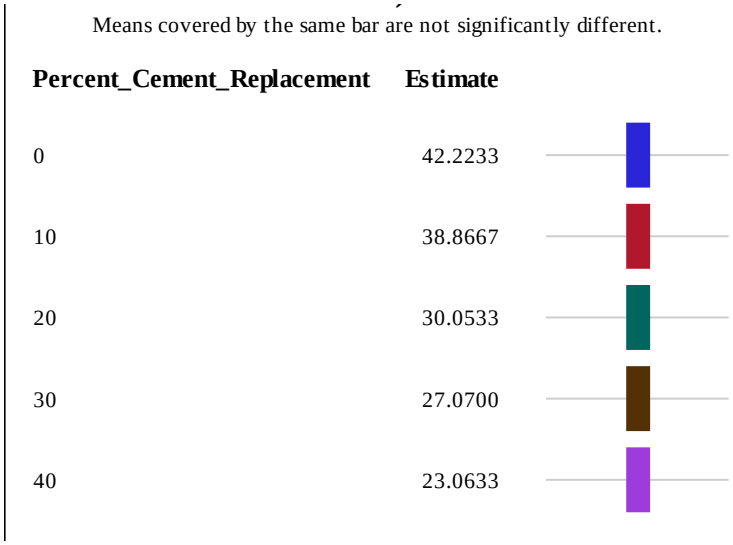

Figure B1. Class-A concrete cylinders 28 days compressive strength Tukey Grouping for Means of Index ($\alpha = 0.05$).

Table B2. Class-A concrete cylinders 90 days compressive strength ANOVA results.

Source	DF	Sum of Squares	Mean Square	F Value	Pr > F
Model	4	524.3124	131.0781	83.49	<.0001
Error	10	15.7002	1.5700		
Corrected Total	14	540.0127			

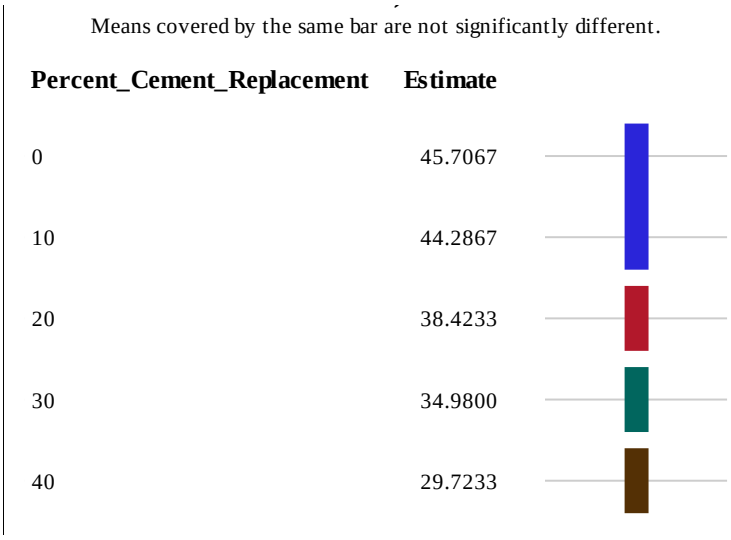

Figure B2. Class-A concrete cylinders 90 days compressive strength Tukey Grouping for Means of Index ($\alpha = 0.05$).

APPENDIX C: STATISTICAL ANALYSIS OF CONCRETE CYLINDERS COMPRESSIVE STRENGTH (CLASS-B)

Table C1. t-test for Class-B concrete cylinders compressive strength at 28 days.

Description	CO-3	P-3-20
Mean	41.8949	33.5016
Variance	0.8848	1.3160
Observations	3	3
Hypothesized Mean Difference	0.050	
df	4	
t Stat	9.7410	
P(T<=t) one-tail	0.0003	
t Critical one-tail	2.1318	
P(T<=t) two-tail	0.0006	
t Critical two-tail	2.7764	

Table C2. t-test for Class-B concrete cylinders compressive strength at 90 days.

Description	CO-3	P-3-20
Mean	45.4066	39.4564
Variance	10.7059	2.4538
Observations	3	3
Hypothesized Mean Difference	0.0500	
df	4	
t Stat	2.8171	
P(T<=t) one-tail	0.0334	
t Critical one-tail	2.1318	
P(T<=t) two-tail	0.0668	
t Critical two-tail	3.1824	